Report SDSMT/IAS/R-91/02 March 1991

ACQUISITION AND ANALYSIS OF DATA FOR THE NORTH DAKOTA THUNDERSTORM PROJECT

By: Paul L. Smith, Andrew G. Detwiler, John H. Hirsch, L. Ronald Johnson, Fred J. Kopp, James R. Miller, Jr., Harold D. Orville and David L. Priegnitz

Prepared for:

North Dakota Atmospheric Resource Board
P.O. Box 1833
Bismarck, ND 58502

Contract No. ARB-IAS-89-2

Institute of Atmospheric Sciences

South Dakota School of Mines and Technology

501 East. St. Joseph Street

Rapid City, South Dakota 57701-3995

ABSTRACT

Research conducted as part of the North Dakota component of the Federal/State Cooperative Program in Atmospheric Modification Research, funded through NOAA, is summarized. The basic objective of the program is to develop improved techniques for evaluating operational weather modification projects. The North Dakota work concentrates on convective-cloud seeding projects and uses data collected in association with the North Dakota Cloud Modification Project (NDCMP). Participation in the 1989 North Dakota Thunderstorm Project and analysis of the resulting data were important activities during the period of this contract. This report provides brief summaries of progress in the analysis of data from tracer studies of transport and dispersion processes in clouds and of weather radar data, as well as in numerical cloud modeling studies. Analysis of data from earlier field projects also continued.

TABLE OF CONTENTS

TABLE OF CONTENTS (continued)

LIST OF FIGURES

LIST OF TABLES

1. INTRODUCTION

This report summarizes progress in continuing research efforts aimed at developing improved evaluation techniques for operational weather modification programs. This research is part of the Federal/State Cooperative Program in Atmospheric Modification Research (Reinking, 1985) and is funded by NOAA through a cooperative agreement with the North Dakota Atmospheric Resource Board. The research is closely coordinated with the operational North Dakota Cloud Modification Project (NDCMP), which is also managed by the Board. Participants in the North Dakota program, in addition to the Board, have included North American Weather Consultants, the South Dakota School of Mines and Technology (SDSM&T), the University of North Dakota (UND), and Weather Modification, Inc., as well as some NOAA scientists. Previous research carried out by the SDSM&T under the program is summarized in Smith et al. (1985a,b), Doneaud et al. (1986), and Smith et al. (1989a,b; 1990). The present contract covered the period 1 May 1989 - 31 March 1991, but virtually all work under the contract was completed prior to 31 May 1990. The highlight of the effort during this period was participation in the North Dakota Thunderstorm Project (NDTP) field campaign in the summer of 1989, and the preliminary analysis of the resulting data.

Recent scientific emphasis in the North Dakota program has been placed on gaining a better understanding of the transport, dispersion, entrainment, and mixing processes taking place inside convective clouds. This knowledge is needed to understand how glaciogenic seeding agents, dispensed primarily at cloud base in the NDCMP, are delivered to the active supercooled parts of the clouds where they can accelerate the development of precipitation-sized particles through ice processes. The transport processes are also of interest in connection with questions about the mechanisms of hailstone embryo development in feeder clouds and the subsequent transfer of the embryos into the primary hail growth regions. Studies of embryo transport processes were an important objective of the NDTP.

The recent North Dakota investigations have emphasized field experiments using a sulfur hexafluoride (SF_6) tracer gas dispensed into the clouds and airborne SF_6 analyzers to follow the transport and dispersion processes inside them. Simultaneous release of silver iodide (AgI) seeding aerosols provides "tagged" regions containing artificial ice nuclei and thereby permits concurrent investigation of the nuclei activation processes in the clouds. Radar chaff and fluorescent beads were included as additional tracers in the NDTP studies, and the results of releases from ground locations were also investigated with the tracer methods.

An important part of the SDSM&T research during the contract period involved participation in the conduct of the NDTP field experiments and the preliminary analysis of the resulting data.

The analysis of data from earlier tracer experiments carried out in the Dickinson, North Dakota, area in the summer of 1987 continued. Numerical cloud modeling studies were also conducted to aid in explaining the basic transport and dispersion processes. These studies complement the field experiments by attempting to simulate the tracer experiments in order to gain increased understanding of the transport and dispersion processes throughout the full volume of the clouds. Analyses of earlier weather radar data from the North Dakota region, including the radar data from the 1987 experiments, were also continued.

The next section of this report presents brief summaries of these activities. Copies of some relevant publications, along with abstracts of other documents completed during the period, are included as appendices.

2. RESEARCH ACTIVITIES

2.1 North Dakota Thunderstorm Project

The North Dakota Thunderstorm Project (NDTP) was conducted in the central Dakotas during the summer of 1989. The project Operations Center was located at the Bismarck, ND, airport. Project aircraft and most personnel were based in Bismarck, with Doppler radars located at Bismarck, Center, and New Salem. A substantial fraction of the SDSM&T Institute of Atmospheric Sciences (IAS) staff participated in the NDTP field effort, as did significant contingents from the Universities of Maryland, North Dakota, and Wyoming, the National Center for Atmospheric Research (NCAR), the NOAA Wave Propagation Laboratory, North American Weather Consultants, and the Atmospheric Resource Board. Funding came from several National Science Foundation (NSF) grants as well as the Federal/State Cooperative Program. An NSF Research Experiences for Undergraduates (REU) grant brought 10 university students to the project (Orville, 1989). The REU students were involved in a great variety of project activities, including storm intercept and upper-air (rawinsonde) measurements.

The field project began on 12 June and continued through 22 July 1989. During the field period, this contract provided partial support for the following activities:

Operations Director (P. L. Smith)
Aircraft Coordinator/Data Manager (J. H. Hirsch)
Real Time Cloud Modeling/Forecasting (F. J. Kopp, H. D. Orville)

Other sources of funding provided the rest of the support for the activities mentioned, as well as other SDSM&T contributions to the NDTP field program.

The NDTP field effort was generally regarded as quite successful. Many of the planned experiments were executed numerous times, but a shortage of mature thunderstorm systems with well-defined feeder clouds limited the opportunities for some of the planned tracer experiments. This probably is a reflection of the fact that central North Dakota remained in the grip of drought during the summer of 1989.

Hirsch (1989) compiled a data inventory for the entire project. Copies of the title page and table of contents for this document appear in Appendix A. He also completed runs of the Hirsch one-dimensional, steady-state cloud model for all NDTP project days, using the Bismarck 00 and 12 UTC soundings as input. The most widespread severe convection occurred on 28 June 1989, and data from that day are being investigated by many NDTP participants. Orville et al. (1990a) presented an analysis of the development of ice particles in some of the vigorous clouds on that day at the 1990 Conference on Cloud Physics.

Radar, aircraft, and cloud-to-ground lightning data from a band of storms on 17 July 1989 have been examined by Detwiler et al. (1990). They observed a total flash rate at least an order of magnitude greater than the cloud-to-ground flash rate recorded by the National Lightning Detection Network. Both total and cloud-to-ground flash rates increased as elements in the band became invigorated and echo tops rose, and decreased when convective activity declined. Lightning flash rate thus appears to be a useful relative indicator of the intensity of convection in a storm. The electic fields measured in-situ during aircraft penetrations of this band are consistent in sign with generally accepted charge-separation mechanisms thought to be active in thunderstorms. This agreement lends support to the use of rate of electrification as an indicator of the rate of precipitation formation in thunderstorms.

Kopp et al. (1990) analyzed the effect of an improved treatment of radiational heating at the surface on the initiation of convection in the SDSM&T two-dimensional, time-dependent cloud model as well as on the forecasting of maximum surface temperatures with this model. A copy of their paper appears in Appendix B. Real-time forecasts of convective activity were made daily from this model during the NDTP, and they have been reviewed by Kopp and Orville (1990). They estimate about 75% success rate in predicting the scale of convection with these experimental forecasts. Appendix C provides a copy of the Kopp and Orville paper.

Universal-format radar data tapes have been generated at the National Center for Atmospheric Research (NCAR) from the CP-3 and CP-4 data for selected NDTP periods; 65 such tapes have been received to date at the SDSM&T. A number of these tapes have been processed and used with the IRAS software (see Section 2.3) to support a variety of research efforts. An M.S. thesis project underway at the SDSM&T will combine an analysis of radar and aircraft data from storms on 6 and 7 July 1989 with numerical model simulations of the clouds observed on those days. The Doppler velocity data fields for three volume scans on 17 July 1989 have been edited and synthesis of the dual-Doppler wind fields using the NCAR-developed CEDRIC software is underway. A second M.S. thesis project in progress at the SDSM&T (with NSF support) involves a dual-Doppler radar analysis of the 17 July squall line.

Some of the analyses mentioned in the preceding paragraphs are being carried out with support from both the Federal/State Cooperative Program and the NSF. Other research supported specifically by NSF grants related to the NDTP includes an analysis of a 28 June 1989 storm with an anomalously high frequency of positive cloud-to-ground lightning flashes (Helsdon, 1990). An analysis of particle sampling statistics applicable to airborne and other sensors (Smith and Liu, 1990) was reported at the 1990 Conference on Cloud Physics. A survey of model simulations of cloud-seeding effects was presented at the 1990 annual meeting of the American Association for the Advancement of Science (Orville et al., 1990b).

2.2 Studies of Transport and Dispersion Processes

Studies were initiated in the North Dakota program in 1984 to investigate in more detail the transport and dispersion of seeding materials inside convective clouds. This is an important link in the chain of events hypothesized to lead to modification of the precipitation from such clouds through cloud-base seeding treatments. The experimental approach adopted was the use of SF_6 tracer gas, released from a treatment aircraft, and sampling aircraft equipped with fast-response SF_6 analyzers to follow the transport and dispersion processes in the clouds. Concurrent release of seeding aerosols along with the SF_6 also provides information about the ice-nuclei activation processes. Key results of the 1984, 1985, and 1987 tracer experiments are summarized by Stith et al. (1986), Stith and Benner (1987), Stith and Politovich (1989), and Stith et al. (1990).

In the 1987 field project, an attempt was made to obtain more complete information about the distribution of the tracer in the clouds, through the use of two sampling aircraft (the UND Citation and the SDSM&T T-28) equipped with SF_6 analyzers. This made it possible to explore the clouds at different levels simultaneously as well as to investigate larger cloud systems. The best coordinated tracer experiment occurred on 28 June 1987, when SF_6 and AgI were released at the base of a moderate-sized, isolated towering cumulus cloud. Stith et al. (1990) provide a good summary of the observations from this case. Huston's (1989) thesis, completed during this contract period, provides some further analysis of aircraft and radar observations from this case, as well as comparisons with results from 1D and 2D model simulations of the cloud.

Comparisons between the model results and observations show that the model cloud tends to be wetter, with maximum model cloud water concentrations about twice the highest values measured by aircraft. The model cloud also develops and produces precipitation, and then decays, over a period of time amounting to approximately 1/3 the estimated lifetime of the observed cloud. However, the model cloud transports tracer material and seeding agent, and develops precipitation, in exactly the same pattern and through the same mechanisms as the observed cloud. Experiments with the model involving natural and seeded precipitation development suggest that seeding cumulus congestus clouds with ice nuclei at cloud base can be an effective means of accelerating precipitation formation and increasing the amount of precipitation that reaches the ground. The seeding must occur prior to natural ice formation in the cloud, and the cloud must last long enough to develop precipitation.

Huston also compared the development of precipitation in this cloud with the precipitation processes in HIPLEX-1 clouds, as reported by Cooper and Lawson (1984). The results from Huston's thesis have been consolidated into a manuscript that was recently accepted for publication in the Journal of Applied Meteorology (Huston et al., 1991). A copy of the abstract of this manuscript appears in Appendix D.

2.3 Radar Data Analysis

The analysis of radar data from both the NDTP and earlier projects has been greatly facilitated by the IRAS software package that was developed during this contract period. This package permits manipulation of radar data on PC-type work stations. A user-oriented manual has been prepared to document the main features of the package, and a condensed description appears in Priegnitz (1991). Appendix E contains copies of the title and header pages from this manual. The IRAS package has been ported to users at the University of North Dakota and elsewhere. The package is also used extensively in SDSM&T radar analysis efforts, as illustrated by some of the examples below.

2.3.1 NDTP Doppler radar analysis

A dual-Doppler radar analysis of a squall line that developed within the NDTP network on 17 July 1989 is underway. The analysis concentrates on the developing phase of this storm, and Fig. 1 illustrates the initial results. The figure shows data for two times (1358 and 1423 CDT). At the earlier time, the echoes are discontinuous and not aligned; several distinct 30 dBz contours can be seen. In contrast, at 1423 a solid line of echo >30 dBz extends from near the northern edge of the analysis region to near the southern edge. Horizontal-velocity vectors reveal the effects of the changing storm morphology. At 1358, air is able to pass through the gaps between storms near Y = 10 and Y = 22 in the figure; less complete penetration is possible at 1423. Also visible to the west of the storm echoes in the figure is a boundary which overtakes the storms. One topic of investigation is the origin of this boundary and its possible role in transforming the broken area of storms into a squall line.

2.3.2 Analysis of 1987 CHILL radar data

Analysis of the CHILL radar data collected at Dickinson in 1987 has continued. Part of the work involves locating first echoes in the data set. Volume scans were recorded approximately every 3 minutes. Another 132 first echoes have been identified and added to the set of 33 reported in Smith et al. (1990); these now include data from 16, 18, and 22 June 1987. Table 1 summarizes the results. The 00 UTC Bismarck sounding was used to assign to the daily mean FEH a corresponding temperature value. The reported 0°C level is based on interpolation of field project soundings taken at Dickinson.

Most first echoes appear above the 0°C level but some are lower; the minimum height is below the 0°C level for each of the three days. Thus some mechanism is operating to produce first echoes below the freezing level. Work is now underway to locate the first echoes for 28 June, 29 June, and 4 July 1987, and to compare all first-echo heights with corresponding Dickinson and Bismarck soundings to determine the individual first-echo temperatures.

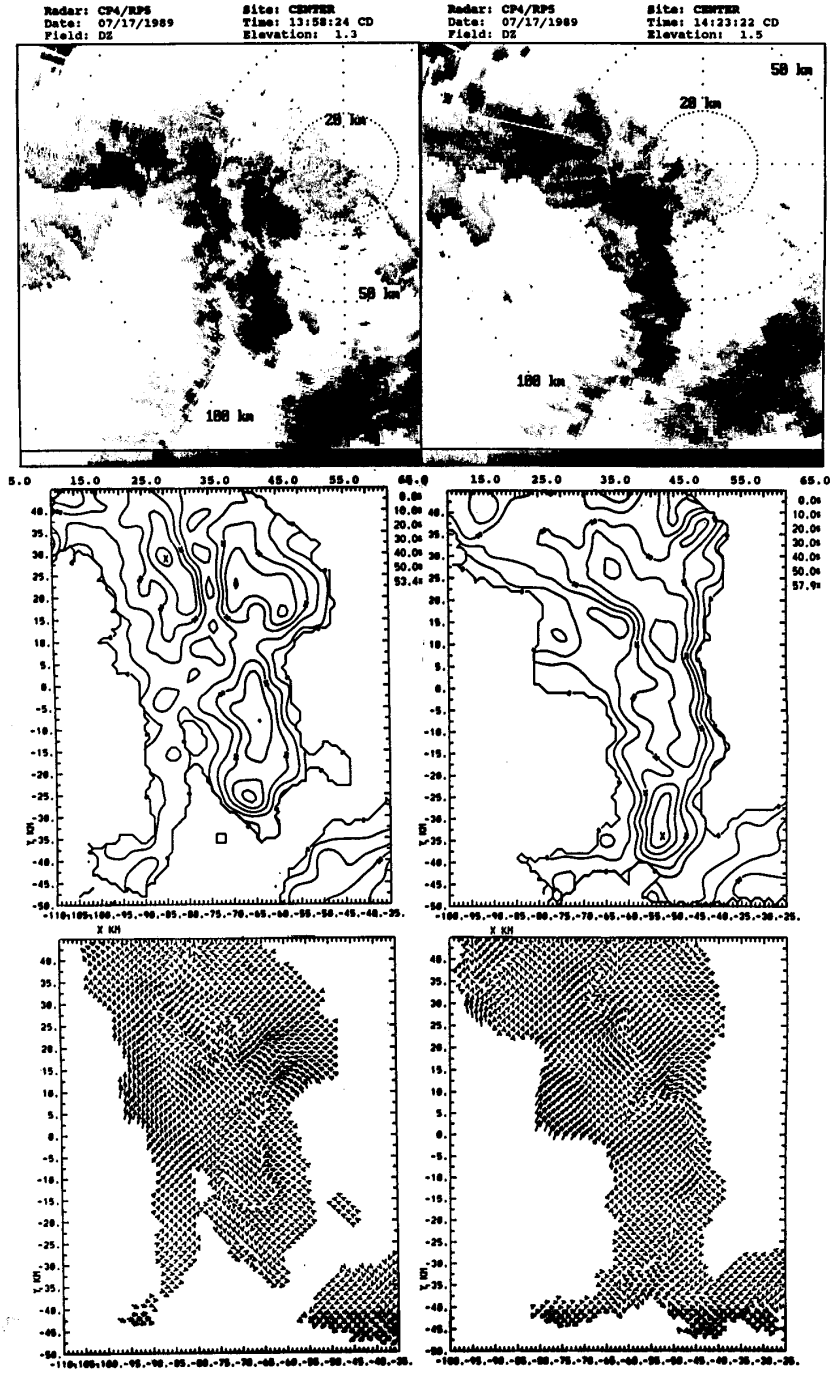

Fig. 1: Sample of radar data for 17 July 1989 storm. (Top panels) plots of radar reflectivity from CP-4 made on the IRAS system (Priegnitz, 1991); (middle panels) gridded and contoured reflectivity data at 2 km AGL from CP-3 and CP-4, combined using the NCAR CEDRIC program (Mohr et al., 1986); (bottom panels) horizontal winds for the two times derived from the radial winds from the two radars; the synthesis was done using the CEDRIC program.

TABLE 1

First-Echo Height and Temperature (daily mean)
for Three Days in June 1987

Date	No. of Echoes	Minimum FEH (km)	Maximum FEH (km)	Mean FEH (km)	Standard Deviation (km)	0°C Level (km)	Temp. at Mean FEH (°C)
16	34	4.40	7.70	6.32	0.88	4.6	-14.0
18	64	3.70	6.60	5.00	0.54	4.0	- 6.0
22	67	3.50	8.50	5.98	1.11	4.95	-11.8
Composite							
	165	3.50	8.50	5.67	1.03		

Accompanying the 1987 CHILL data were routines written by the Illinois State Water Survey to read the tapes and retrieve the Doppler velocity fields in units of meters per second. Software was developed to reduce the data quantity for easier manipulation, since a full volume scan requires approximately 20 MB of disk space. When only values for the stormy regions are of interest, the first compression technique thresholds out most of the noise and the clear-air returns by selecting only bins with reflectivities greater than a specified threshold (normally 8 dBz). Doppler data for 1744 through 1820 MDT on 22 June 1987 have been processed and transferred to the PC format compatible with IRAS. The UND Citation made cloud penetrations following a SF_6 release north of the radar site during this period. The Citation flight track from 18:00 to 18:16 is superimposed on the reflectivity (>14 dBz) pattern recorded at 18:13:43 by CHILL in Fig. 2. The Doppler data demonstrate some local convergence early in the case lifetime and the later effect of the ambient environmental flow as the cloud drifted off to the north/northeast.

2.3.3 Area-time-integral analysis

Assessment of the utility of the Area-Time-Integral (ATI) method for estimating convective rainfall continues. Results using various combinations of predictor relationships between the ATI and rainfall amounts (e.g., derived from the North Dakota or CCOPE observations) and predictand values were reported at the 8th Conference on Hydrometeorology (Johnson and Smith, 1990). Appendix F contains a copy of that paper.

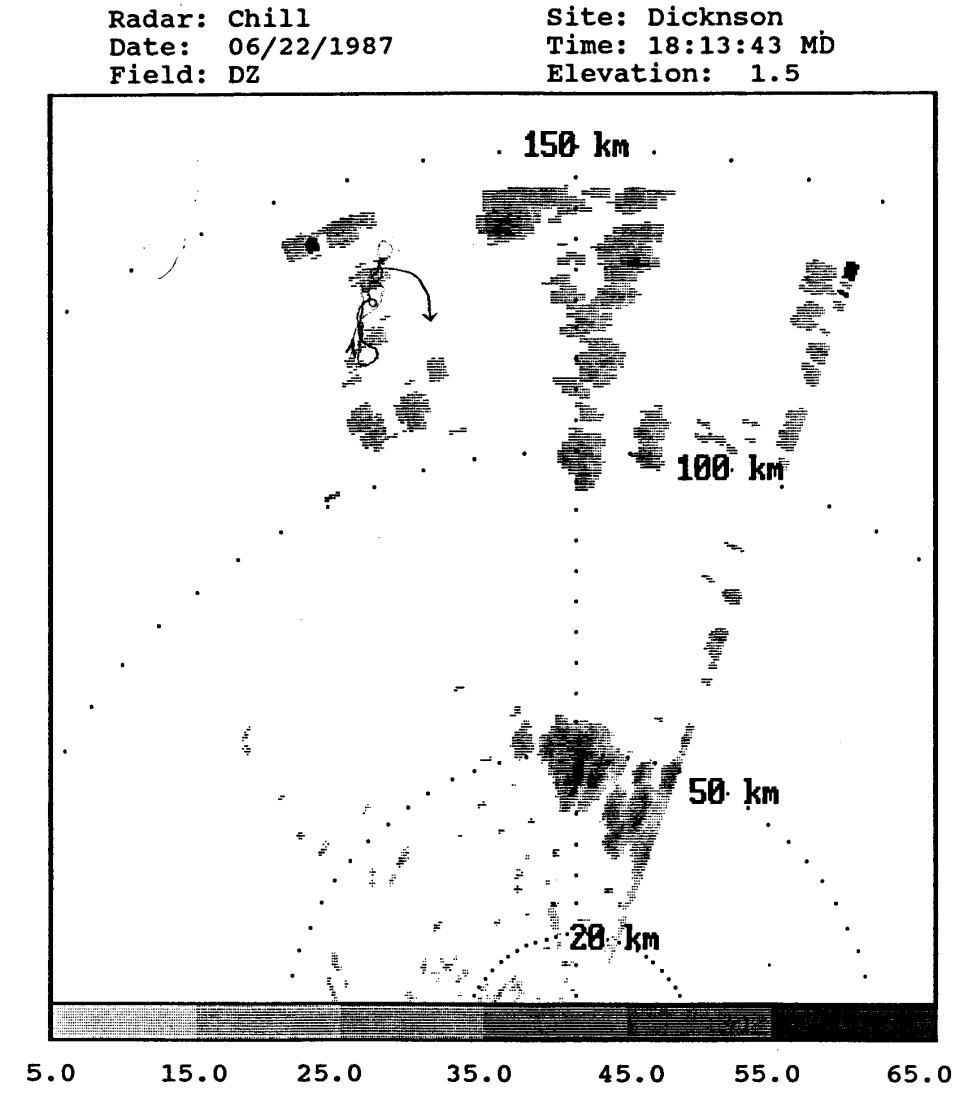

Fig. 2: Slant-PPI sector scan for 1814 MDT on 22 June 1987, with 6 min of Citation flight track superimposed. Reflectivity gray scale in dBz is indicated at bottom.

Rain volumes from radar echo clusters are related to the corresponding ATI values by a power-law relation of the form $V = k(ATI)^b$, where k and b are constants determined by regression analysis. Table 2 compares k and b values for past years from North Dakota, CCOPE, FACE, and COHMEX using three different types of radar. Good reproducibility has been found for the same radar in the same location. Some evidence of geographic transferability is apparent, but equipment-related differences appear to have the largest impact.

TABLE 2

ATI-Rainfall Volume Parameters Determined by Regression Analysis for Several Different Projects and Radars

PROJECT (Year)	k	b	RADAR TYPE
NDPP (1972)*	2.62	1.09	S-band, 2° beam
NDCMP (1980)	3.68	1.01	C-band, 2° beam
NDCMP (1981)	3.07	1.08	C-band, 2° beam
NDCMP (1982)	3.74	1.02	C-band, 2° beam
NDCMP (1984)	3.57	1.03	C-band, 2° beam
CCOPE (1981)	2.12	1.09	C-band, 1° beam
FACE (78, 79, 80)	3.40*	1.00	S-band, 2° beam
COHMEX (1986)	3.78	1.10	S-band, 2° beam

*18-dBz threshold used for ATI; all others used 25 dBz threshold.

2.3.4 CCOPE radar echo cluster statistics

A radar echo climatology from CCOPE (carried out in eastern Montana in 1981), developed initially under other sponsorship (Tao, 1987; Doneaud and Johnson, 1987), was completed and published (Johnson and Hjelmfelt, 1990). A copy of that paper appears in Appendix G. The extensive CCOPE data are relevant to this project because the climatology of southeastern Montana is quite similar to that of the NDCMP districts in western North Dakota. The CCOPE data were collected with a C-band radar having 1° beamwidth, which provides a useful comparison with the 2° radars used in the North Dakota Federal/State Cooperative Program field projects up through 1984.

The average CCOPE echo cluster was initiated in the mid-afternoon (15:18 MDT) and continued for 1.8 hours. It had a maximum reflectivity of 45.4 dBz and produced 296 $km^2 \cdot mm$ of rainfall. The storm moved from west to east at a speed of 12.5 m s^{-1}. These results are generally consistent with those obtained for the North Dakota project for the same year (Smith et al., 1985a). This suggests that the results are applicable and transferable to the broader northern Great Plains area.

Analysis revealed a bimodal distribution of maximum echo heights, with the low mode centered at 6.9 km and the upper mode at 9.4 km (Fig. 3). A similar characteristic was noted in the radar data from METROMEX. To our knowledge, the bimodal distribution of maximum echo heights observed in the present study has not been reported previously for High Plains storms. The North Dakota observations (with 2° beamwidths) have shown only a single mode (e.g., Smith et al., 1985b). The implications of the results of the modeling study by Mueller (1978) suggesting that METROMEX clouds could be moved from the lower mode to the higher mode as a result of enhanced glaciation are especially intriguing.

The usefulness of the Area-Time Integral (ATI) in estimating total storm rainfall was reaffirmed for this CCOPE data set. On the other hand, maximum echo height was found not to be as good an estimator of rainfall as was indicated in previous studies (Smith et al., 1985a,b). Perhaps the better resolution provided by the 1° beamwidth of the CCOPE radar data used here is a factor.

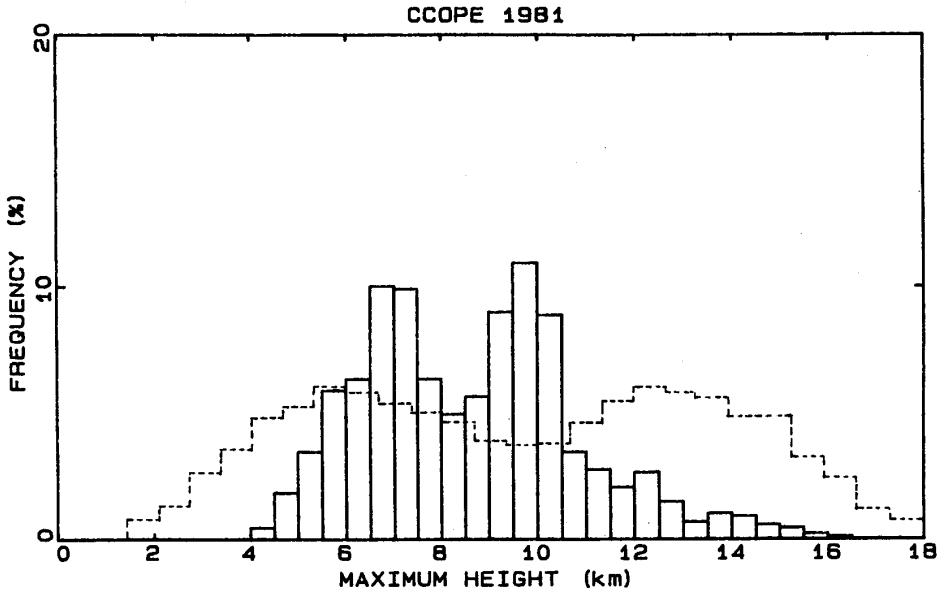

Fig. 3: Frequency distribution of CCOPE maximum echo height, using 1/2 km bin width. Dashed line for St. Louis clouds, adapted from Braham (1981).

2.4 Rainfall Analysis

An analysis of rainfall data from the North Dakota volunteer observer network has been initiated. The first efforts involve conducting a climatological analysis and looking for any evidence of seeding effects in the North Dakota Cloud Modification Project (NDCMP) target areas. A simulation of a randomized seeding experiment using data from a section of the state where no actual seeding operations have been conducted is also under consideration. The objective would be to look for any artifact indications of seeding effects, which might arise from inherent characteristics of regression analysis.

2.5 Numerical Cloud Modeling Studies

2.5.1 Sounding cross-section analysis

The sounding data sets for Elgin (EGN), Bismarck (BIS), and Goodrich (GDH) were examined to determine times at which the three sites may have had simultaneous balloon releases. Only one such day existed in the data set, and that was on the 29th of June at 0000 GMT. These soundings were plotted on skew-T diagrams and then combined as a cross section (see Fig. 4). The cross section shows each sounding

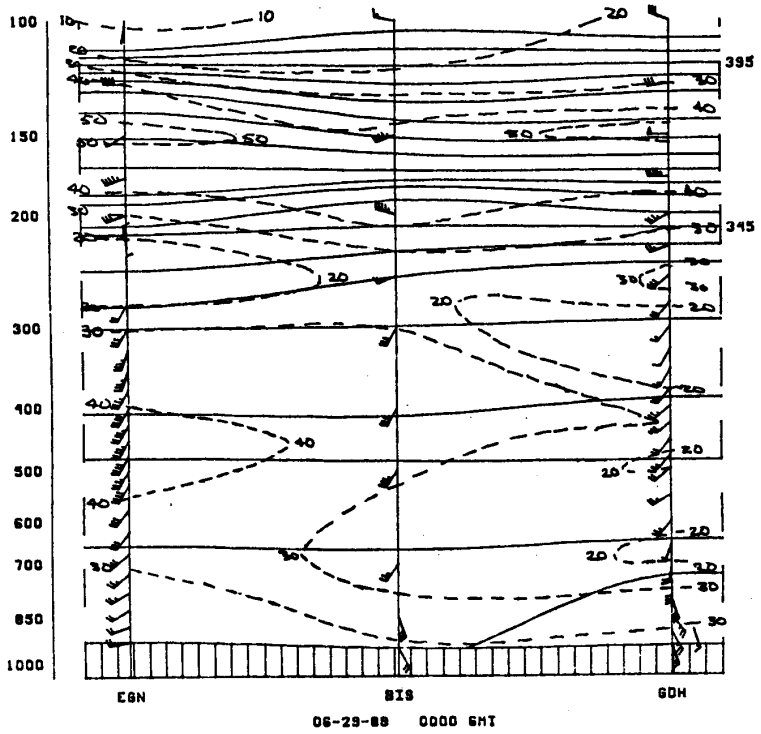

Fig. 4: Vertical cross-sectional analysis at 0000 GMT, 29 June 1989. Solid lines are ϑ_e; equivalent potential temperature (°K); dashed lines are wind speed (kts).

location spaced relative to one another with the ground elevation in blocks along the bottom. The vertical axis is atmospheric pressure in millibars decreasing upward.

Sounding data from each site were then analyzed. In Fig. 4, the winds are plotted in the standard meteorological format with an isotach analysis shown as dashed lines. A general southwesterly flow occurs throughout the region from the surface to near 200 mb. The surface winds at BIS and at GDH indicate low level convergence to approximately 750 mb with southeasterly flow at speeds 25 to 30 kts, thus placing the area of convergence to the west of Bismarck at the sounding time of 0000 GMT.

Solid lines in the figure represent an analysis of θ_e, equivalent potential temperature in °K. The analysis shows a relatively unstable atmosphere which extends from the surface to near 200 mb.

The combination of low level convergence, instability of the tropospheric layer, and the flux of moisture from the southeasterly flow (not shown here) produced a squall line of severe thunderstorms. Hailstones with diameters of 1.5 inches fell within a 50 nm radius of Bismarck from this well organized weather system. The squall line was preceded by a gust front that moved at speeds close to 60 kts as it passed Bismarck at approximately 0130 GMT.

2.5.2 Model simulation of parcel trajectories

The SDSM&T two-dimensional, time-dependent cloud model has been modified to provide outputs indicating the trajectories of selected air parcels through the model domain. This capability will permit more direct comparisons between model results and tracer experiments such as those discussed in Section 2.2.

Positions of 25 air parcel trajectories have been traced in the simulation of the 28 June 1987 experiment. The treatment and the trajectories were initiated at 84 minutes of simulated time. Initially the parcels were in a square 5 x 5 grid with spacing of 200 meters. Parcel positions are plotted for each succeeding minute, for about 6 minutes, in Fig. 5. Comparing the "seeding-agent" field at 91 minutes (Fig. 6) with the plot of parcel trajectories starting at 84 minutes shows similar diffusion.

More interesting results appear in the plot of air parcel trajectories starting at 91 minutes (Fig. 7). There are some loops in the trajectories, indicating the possibility of particle recirculation processes. The parcels that have moved the greatest distance from the starting point are tracing out a downshear divergence region. This region can be seen in the "seeding-agent" field at 99 minutes (Fig. 8) as the right-hand closed contours of agent concentration.

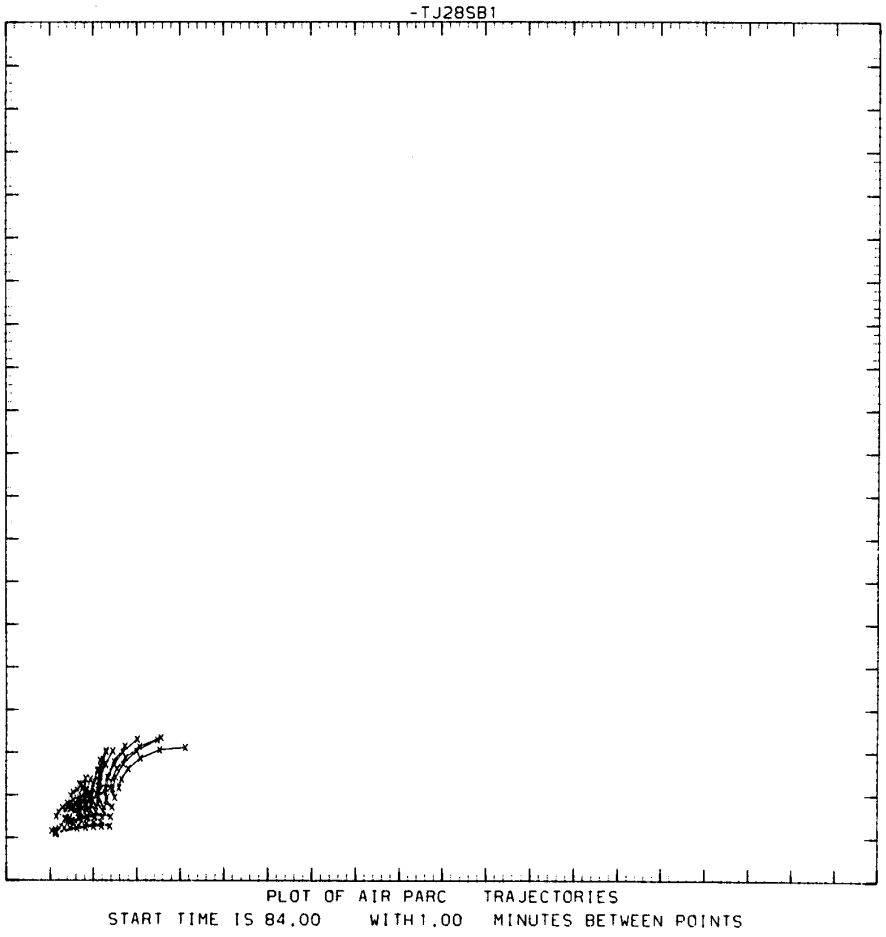

Fig. 5: Example of parcel trajectories in the two-dimensional, time-dependent cloud model simulation of the 28 June 1987 North Dakota tracer experiment. Plot shows vertical-section model domain, 20 x 20 km. Trajectories begin at time of treatment initiation (84 min of model time) and x's mark 1-min intervals along each trajectory.

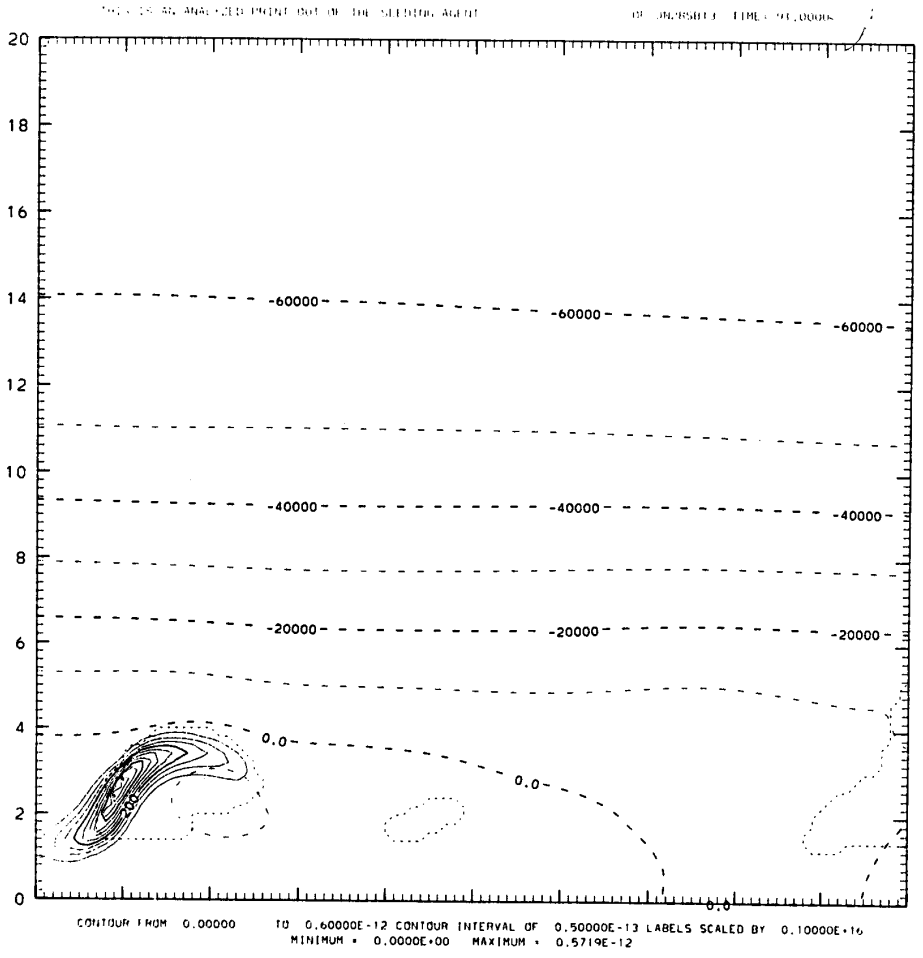

Fig. 6: Contoured field of treatment-agent concentration over the 20 x 20 km vertical-section model domain at 91 min of model time (7 min after treatment initiation). Dashed lines indicate streamlines.

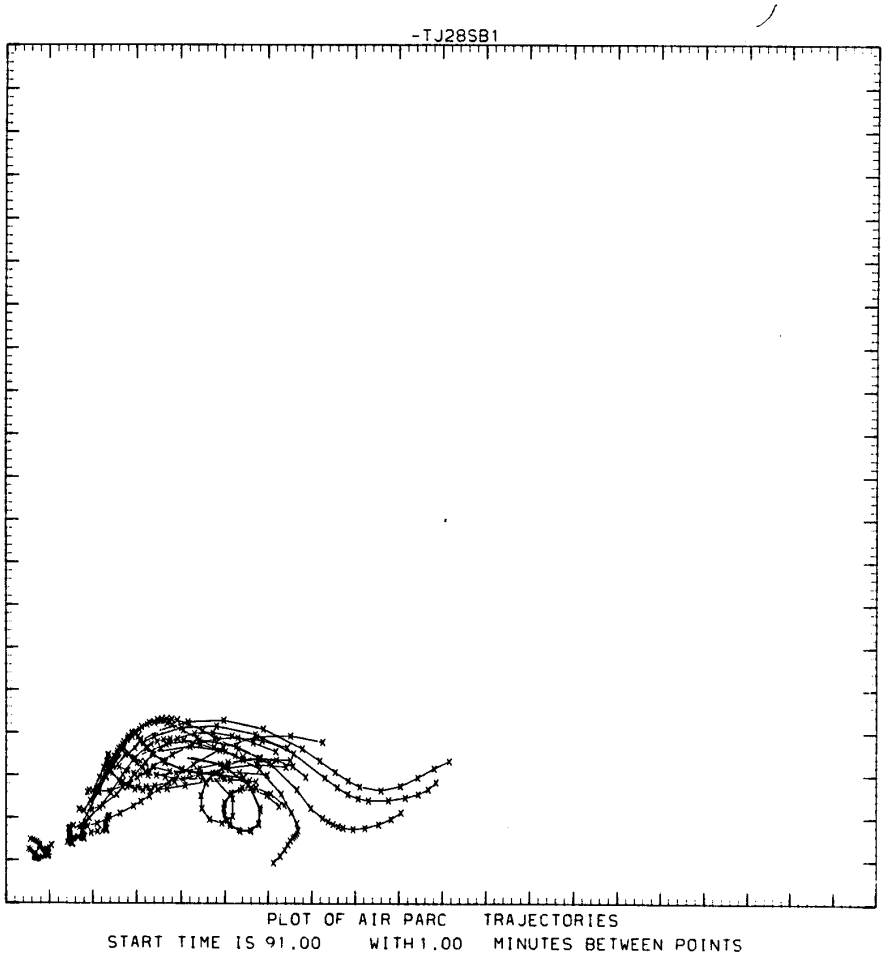

Fig. 7: As Fig. 5, but with trajectories initiated at 91 min of model time and continuing for 12 min.

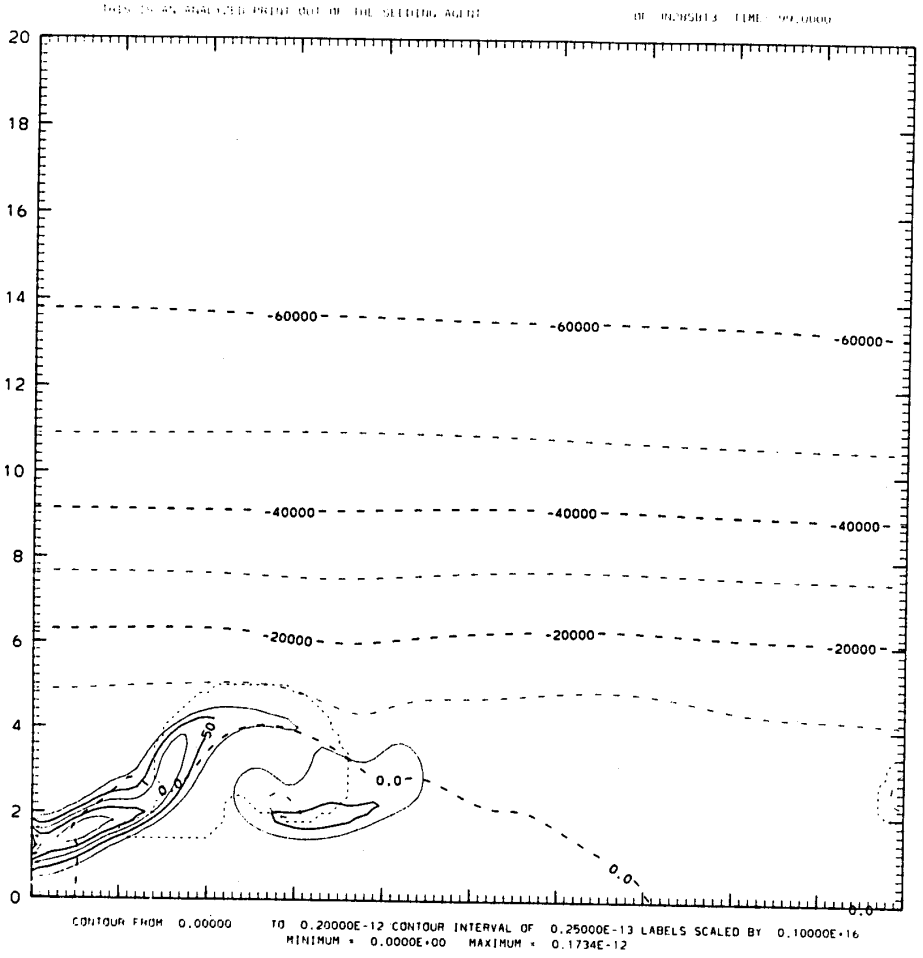

Fig. 8: As Fig. 6, but showing conditions at 99 min of model time (8 min after the trajectories in Fig. 7 were initiated).

There are too many parcel trajectories in a small region to trace particular ones from the beginning to the end in this particular example. It is also evident that some means will be needed to compensate for the cloud drift if direct comparisons with the aircraft tracer experiments are to be made.

2.6 Other Investigations

In the 1987 project at Dickinson, volume scans of clouds were made with a dual-wavelength microwave radiometer. An analysis of those volume scans completed by Anantharaj (1989) is being prepared for publication. The abstract of his thesis appears in Appendix H.

As noted in Sec. 2.3, a manual on the Interactive Radar Analysis Software (IRAS) package developed to support interactive display and analysis of radar data from the various North Dakota field projects was prepared (see Appendix E). This software operates on a PC computer system, although means to download the radar data into the computer are necessary. The package has been enhanced to include vertical cross sections along user-defined line segments. In addition, the PPI/CAPPI interrogation function now displays the data sample time and bin height, and the code has been modified to improve display times. A paper describing IRAS capabilities was presented at the 7th International Conference on Interactive Information and Processing Systems (IIPS; Priegnitz, 1991).

A radar conference panel report on precipitation measurement and hydrology, compiled previously with support under the Federal/State Cooperative Program, was also published this year (Smith, 1990).

ACKNOWLEDGMENT

This research was sponsored by the NOAA-North Dakota Cooperative Agreement NA89RAH09088, Federal-State Cooperative Program in Atmospheric Modification Research under Contract No. ARB-IAS-89-2.

REFERENCES

Anantharaj, V. G., 1989: An exploratory study of the summertime observations by a dual-wavelength microwave radiometer at Dickinson, North Dakota in 1987. M.S. Thesis, Dept. of Meteorology, S.D. School of Mines and Technology, Rapid City, SD. 116 pp.

Braham, R. R., Jr., 1981: Urban precipitation processes. In Changnon, S. A., ed. METROMEX: A review and summary. Meteor. Monogr., 40, 76-116.

Cooper, W. A., and R. P. Lawson, 1984: Physical interpretation of results from the HIPLEX-1 experiment. J. Climate Appl. Meteor., 23, 523-540.

Detwiler, A. G. J. H. Helsdon, Jr., and D. J. Musil, 1990: Evolution of a band of severe storms. Preprints Conf. Atmos. Elec., Kananaskis Provincial Park, Alberta, Canada, Amer. Meteor. Soc., 705-709.

Doneaud, A. A., and L. R. Johnson, 1987: Climatological studies of the radar echoes during CCOPE. Preprints 3rd Conf. Mesoscale Processes, Vancouver, B.C., Canada, Amer. Meteor. Soc., 21-26 Aug 1987.

_____, R. D. Farley, M. J. Fuhs, J. H. Hirsch, A. Makarau, J. R. Miller, Jr., H. D. Orville, P. E. Price and P. L. Smith, 1986: Development of evaluation techniques for operational convective cloud modification projects: 1985-86 studies. Report SDSMT/IAS/R-86/05, Institute of Atmospheric Sciences, S.D. School of Mines and Technology, Rapid City, SD. 44 pp.

Helsdon, J. H. 1990: Analysis of a high positive-flash frequency severe storm (28 June 1989) from the North Dakota Thunderstorm Project. Preprints Conf. Atmos. Elec., Kananaskis Provincial Park, Alberta, Canada, Amer. Meteor. Soc., 744-745.

Hirsch, J. H., 1989: North Dakota Thunderstorm Project: 1989 Field Program Data Inventory. Bulletin 89-5, Institute of Atmospheric Sciences, SD School of Mines and Technology, Rapid City, SD.

Huston, M. W., 1989: One- and two-dimensional model results compared with observations from a North Dakota cloud. M.S. Thesis, Dept. of Meteorology, S.D. School of Mines and Technology, Rapid City, SD. 89 pp.

_____, A. G. Detwiler, F. J. Kopp and J. L. Stith, 1991: Observations and model simulations of transport and precipitation development in a seeded cumulus congestus cloud. [Accepted for publication J. Appl. Meteor.]

Johnson, L. R., and M. R. Hjelmfelt, 1990: A climatology of radar echo clusters over southeastern Montana. J. Wea. Modif., 22, 49-57.

_____, and P. L. Smith, 1990: Estimation of convective rain volumes utilizing the area-time-integral technique. Preprints 8th Conf. on Hydrometeor., Kananaskis Provincial Park, Alberta, Canada, Amer. Meteor. Soc., 165-168.

Kopp, F. J., and H. D. Orville, 1990: The use of a cloud model to predict convective and stratiform clouds and precipitation. Preprints 16th Conf. Severe Local Storms, Kananaskis Provincial Park, Alberta, Canada, Amer. Meteor. Soc., 322-327.

_____, _____, J. A. Jung and R. T. McNider, 1990: A parameterization of radiation heating at the surface in a numerical cloud model. Preprints Conf. Cloud Physics, San Francisco, CA, Amer. Meteor. Soc., J81-J84.

Mohr, C. G., L. J. Miller, R. L. Vaughn and W. Frank, 1986: The merger of mesoscale datasets into a common cartesian format for efficient and systematic analyses. J. Atmos. Ocean Tech., 3, 144-161.

Mueller, S. F., 1978: An application of the Simpson-Wiggert cloud model to METROMEX Hi-Cu data. Preprints Conf. Cloud Physics and Atmos. Electricity, Issaquah, WA, Amer. Meteor. Soc., 490-495.

Orville, H. D., 1989: A report on the Conference on the Science and Technology of Cloud Seeding in the Black Hills. J. Wea. Modif., 22, 158-162.

_____, F. J. Kopp, U. S. Nair, J. L. Stith and R. Rinehart, 1990a: On the origin of ice in strong convective cells. Preprints Conf. Cloud Physics, San Francisco, CA, Amer. Meteor. Soc., 16-20.

_____, R. D. Farley and F. J. Kopp, 1990b: The simulation of cloud seeding effects using numerical cloud models. Presented Annual Meeting of the American Association for the Advancement of Science, New Orleans, LA, 15-20 Feb 1990.

Priegnitz, D. L., 1991: The interactive radar analysis software (IRAS) package. Proc. 7th Intnl. Conf. Interactive Information and Processing Systems (IIPS) for Meteor., Oceanography, and Hydrology, 71st AMS Annual Meeting, 13-18 Jan 1998, New Orleans, LA, --.

Reinking, R. F., 1985: An overview of the NOAA Federal-State Cooperative Program in Weather Modification Research. Proc. 4th WMO Sci. Conf. Wea. Modif., Geneva, Switzerland, 643-649.

Smith, P. L., (as Panel Chairman), 1990: Panel response: Precipitation measurement and hydrology. In Radar in Meteorology (D. Atlas, ed.) Amer. Meteor. Soc.

_____, and Z. Liu, 1990: Some statistics of sampling from exponential particle size distributions. Preprints 1990 Conf. Cloud Physics, San Francisco, CA, Amer. Meteor. Soc., 367-370.

_____, A. A. Doneaud, J. H. Hirsch, J. R. Miller, Jr., and P. E. Price, 1985a: Development of evaluation techniques for operational convective cloud modification projects: 1984-85 studies. Report SDSMT/IAS/R-85/05, Institute of Atmospheric Sciences, S.D. School of Mines and Technology, Rapid City, SD. 34 pp.

_____, J. R. Miller, Jr., A. A. Doneaud, J. H. Hirsch, D. L. Priegnitz, P. E. Price, K. J. Tyler and H. D. Orville, 1985b: Research to develop evaluation techniques for operational convective cloud modification projects. Report SDSMT/IAS/R-85/02, Institute of Atmospheric Sciences, S.D. School of Mines and Technology, Rapid City, SD. 93 pp.

_____, L. R. Johnson and F. J. Kopp, 1989a: Development of evaluation techniques for operational convective cloud modification projects: 1986-87 studies. Report SDSMT/IAS/R-89/02, Institute of Atmospheric Sciences, S.D. School of Mines and Technology, Rapid City, SD. 15 pp. + appendices.

_____, M. W. Huston and L. R. Johnson, 1989b: Development of evaluation techniques for operational convective cloud modification projects: 1987-88 studies. Report SDSMT/IAS/R-89/03, Institute of Atmospheric Sciences, S.D. School of Mines and Technology, Rapid City, SD. 13 pp. + appendices.

_____, A. G. Detwiler, J. H. Hirsch, L. R. Johnson, F. J. Kopp, J. R. Miller, Jr., H. D. Orville and D. L. Priegnitz, 1990: Development of evaluation techniques for operational convective cloud modification projects: 1988-89 studies. Report SDSMT/IAS/R-90/01, Institute of Atmospheric Sciences, S.D. School of Mines and Technology, Rapid City, SD. 31 pp. + app.

Stith, J. L., and R. L. Benner, 1987: Application of fast response continuous SF_6 analyzer to in situ cloud studies. J. Atmos. Oceanic Tech., 4, 599-612.

_____, and M. K. Politovich, 1989: Observation of the effects of entrainment and mixing on the droplet size spectra in a small cumulus. J. Atmos. Sci., 46, 908-919.

_____, D. A. Griffith, R. L. Rose, J. A. Flueck, J. R. Miller, Jr., and P. L. Smith, 1986: A preliminary study of transport, diffusion and ice activation in cumulus clouds using an atmospheric tracer. J. Climate Appl. Meteor., 25, 1959-1970.

_____, A. G. Detwiler, R. F. Reinking and P. L. Smith, 1990: Investigating transport, mixing, and the formation of ice in cumuli with gaseous tracer techniques. Atmos. Res., 25, 195-216.

Tao, Ningsheng, 1987: Some radar echo characteristics during CCOPE. M.S. Thesis, Dept. of Meteor., SD School of Mines and Technology, Rapid City, SD. 102 pp.

APPENDIX A

North Dakota

Thunderstorm Project

1989 FIELD PROGRAM

DATA INVENTORY

Edited by John H. Hirsch
Institute of Atmospheric Sciences
South Dakota School of Mines and Technology
Rapid City, South Dakota 57701-3995

December, 1989

Prepared for:
North Dakota Atmospheric Resource Board
P.O. Box 1833
Bismarck, North Dakota 58502
Contract No. ARB-IAS-89-2

TABLE OF CONTENTS

TABLE OF CONTENTS (cont.)

LIST OF FIGURES

LIST OF TABLES

APPENDIX B

Reprinted from the Preprint Volume of the 1990 Conference on Cloud Physics, July 23-17, 1990, San Francisco, Calif. Published by the American Meteorological Society, Boston, Mass.

J2.7

A PARAMETERIZATION OF RADIATION HEATING AT THE SURFACE IN A NUMERICAL CLOUD MODEL

Fred J. Kopp, Harold D. Orville, James A. Jung,[1] and Richard T. McNider[2]

Institute of Atmospheric Sciences
South Dakota School of Mines and Technology
501 East St. Joseph Street
Rapid City, South Dakota 57701-3995

1. INTRODUCTION

A two-dimensional, time-dependent model has been used in a predictive mode during two recent field projects. Initially, the model was tested for its predictive capabilities during the COHMEX project in 1986. During this project, radiative heat flux into the surface layer of the model was parameterized and incorporated. A morning sounding from the Huntsville Redstone Arsenal was used to initialize the model. The simulated heat flux at the surface would heat out the inversion and generate convective clouds. In a second project, the North Dakota Thunderstorm Project in 1989, the model was used in a predictive mode with the output being utilized for briefing purposes.

In the following, we will develop the parameterized radiation heat flux that was incorporated in the model and describe the results from the two experimental attempts at using the model in the predictive mode.

2. CLOUD MODEL

The model is a two-dimensional, time-dependent finite difference grid with 200 m grid spacing. The domain is a 20-km horizontal by 20-km vertical region. Partial differential equations predict air flow, water vapor, cloud water, ice, rain, hail, snow, heat, and other miscellaneous variables. The model is described at greater length in Orville and Kopp (1977) as well as other papers. The critical changes that have been made in this particular model involved changes in the boundary layer heat flux.

The surface energy equation has been modified to change control of surface temperature as used in our past models where the surface temperature was prescribed as a time-dependent change. We now prescribe a constant flux of heat into the surface layer of the model which is also balanced by an eddy transport of heat out of the surface layer.

The energy equation in the model is embodied in the following equation at the surface:

$$\frac{\partial \phi}{\partial t} = -V \cdot \nabla \phi + \frac{2K}{H\theta} \frac{\partial \theta}{\partial z} + \frac{2}{H} K \frac{L}{C_p T_{oo}} \frac{\partial Q}{\partial z} - \frac{2D}{\rho_o C_p H\theta} \quad (1)$$

where the first term on the right is the advection, followed by the vertical diffusion of heat and vapor, and last the radiation heat source.

In the above, ϕ is defined initially as:

$$\phi = \frac{\theta}{\theta} + \frac{Lr}{C_p T_{oo}} \quad (2)$$

where θ is the potential temperature, θ is the deviation of potential temperature from the base state, and r is the mixing ratio. L is the latent heat of vaporization, C_p is heat capacity of air, and T_{oo} is temperature. K is the eddy diffusion coefficient, V is velocity, ρ_o is density, and H is the grid spacing.

The variable D in (1) is the energy flux into the surface layer of height H/2. The energy flux used is about 300 J m^{-2} s^{-1} at the surface. This is a fraction of the short wave solar energy reaching the surface.

In the event that clouds form overhead, the heating rate is reduced to one-half of the original heating rate. This is a very highly parameterized simulation of the radiative flux of the surface. No attempt has been made to simulate long wave radiation interactions at the surface, nor has any attempt been made to simulate the time-dependent short wave variation that occurs as the sun rises, reaches its zenith, and sets.

3. RESULTS

During the COHMEX project, the model was run on some but not all of the days. As seen in Fig. 1,

---

[1]Present Affiliation: James A. Jung, North Dakota Atmospheric Resource Board, P.O. Box 1833, Bismarck, ND 38502.

[2]Present Affiliation: Richard T. McNider, Dept. of Mathematics and Statistics, University of Alabama in Huntsville, Huntsville, AL 35899.

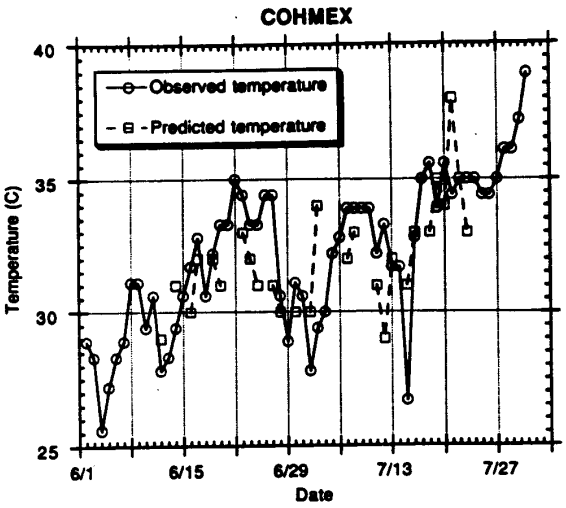

Fig. 1: Observed high temperature for each day of the COHMEX project and the corresponding model predicted temperature.

the model was run on approximately 25 of the 60 days shown in the figure. The model tends to underpredict as well as overpredict temperature. For this particular project, the correlation coefficient for the data shown in the scatter diagram, Fig. 2, was 0.5. The use of the model during this project was largely experimental, with little use made of the model results for the weather briefings. The briefings were held early in the morning before the cloud model could be run. Facilities for displaying model results were limited in any case due to a major failure of part of the McIDAS hardware at the Marshall Space Flight Center.

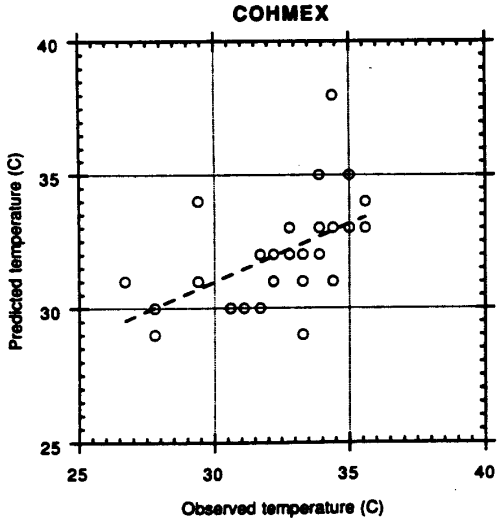

Fig. 2: Scatter plot of COHMEX model predicted vs. observed temperature. The dashed line is a regression line fitted to data. The correlation coefficient is 0.5.

During the North Dakota Thunderstorm Project, the model was used in a predictive mode and the results were intended to be used during the briefings which were held in the late morning. The 12 Z soundings were available at 8:00 local time and were run on the NCAR computer system. Results were generally available by 9:00-10:00 local time with the graphics being downloaded to a microcomputer and printed at the project site.

Figure 3 shows the observed high temperature as well as the predicted temperature for each day during the project. There are three missing data points for predicted temperature as those were declared down days and the model was not run. This figure shows a much closer correlation between the observed temperature and the model predicted temperature. Figure 4 is a scatter diagram of the data and the regression line has a correlation coefficient of > .85. The largest deviation shown in Fig. 3 is approximately 8°C with most of the differences being on the order of 2-3 degrees Celsius.

During the project, a subjective log was kept indicating whether the model had done a good job of predicting cloud development during the day or not. This was generally indicated by making a "+" for a good simulation, a "0" for a fair simulation, and a "-" for a poor simulation. For the 35 days simulated, eight minuses and six zeros were recorded. Figure 5 has this information recorded on it as a +1, 0, or -1. One might expect the big temperature errors made by the model to result in a poor simulation. However, note that 2 July is considered to be a fair day. On the other hand, 8 July, which is a fairly close correlation between predicted and observed temperature, was a minus day, indicating a poor simulation of the cloud growth and, in fact, the model overpredicted the cloud growth on that day. We estimate that the model scored about 75%, for predicting cloud growth, missing about 25% of the time. In some cases, the model did not predict enough cloud growth, but the dominant model result

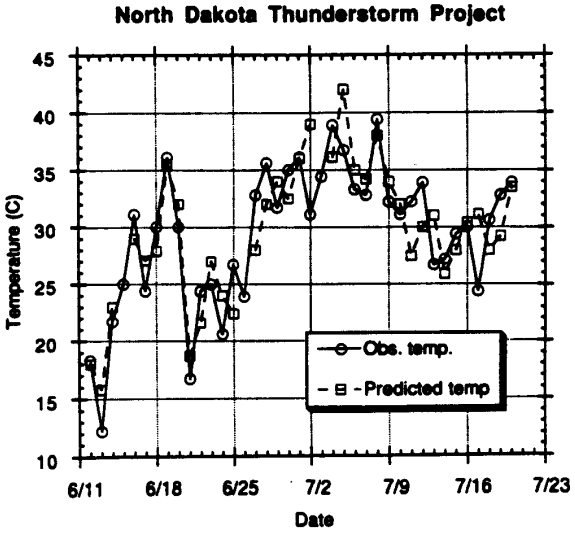

Fig. 3: As in Fig. 1, but for the North Dakota Thunderstorm Project.

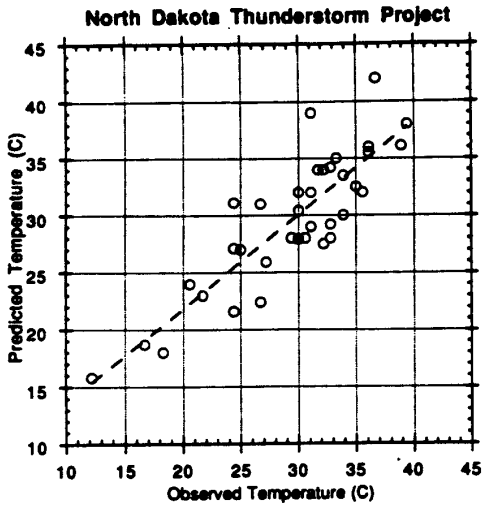

Fig. 4: Scatter plot for the North Dakota Thunderstorm Project of model predicted vs. observed high temperature. The dashed line is a regression line. Correlation of the data is 0.85.

was to predict more cloud growth than actually occurred on the days that the model missed.

Figure 6 shows the precipitable water and the surface mixing ratio from the 12 Z soundings for the project period. The interesting thing to note is that there are substantial changes in both the precipitable water and surface layer mixing ratio. These changes are fairly well correlated with each other. The first few days of the project are characterized by high pressure moving in which led to a drying out of the atmosphere. Subsequent variations are generally related to frontal passages with the accompanying air mass changes. When these changes occur during the day, the initial conditions used from the 12 Z sounding for the model are probably changing rapidly.

4. DISCUSSION

While the model was successful on approximately 75% of the days in predicting the cloud characteristics, the obvious question comes as to why does it fail on the other 25% of the days. During the project, the model was run more than once, frequently with convergence or divergence imposed to get a model response from various synoptic scale effects that were expected to be taking place. In spite of this, we still had failures on 25% of the days and, consequently, the first thought is that the model may be overheating and becoming more convective than the natural convection. An analysis of Fig. 3 related with the failures does not suggest that this is a real problem. In particular, the 2 July difference between the predicted and observed temperature was not a model failure day. Most of the questionable days have only a few degrees difference between the observed and predicted temperature, and there is no difference for the model being either warmer or colder than the observed temperature. There seems to be a general mix of both occurrences. Consequently, a better radiation scheme simulation

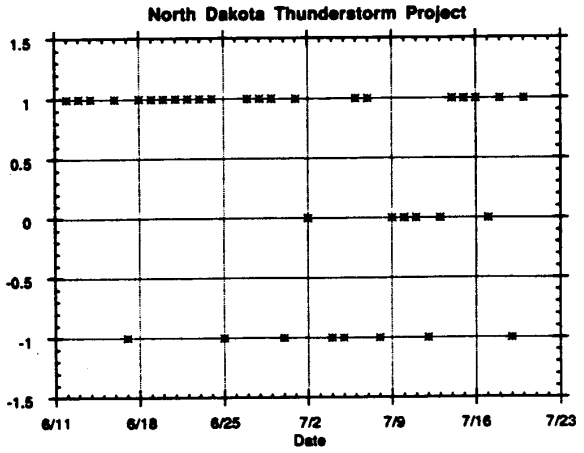

Fig. 5: Plot of day vs. model prediction of cloud characteristics. A "1" indicated good results, "0" is fair, and "-1" is poor.

at the surface would probably not improve the results.

Analysis of Fig. 6 shows that many of the model failures take place on a day when there is high precipitable water and surface moisture but which is followed the next day by a very steep decline in these variables. This suggests that, on some occasions, the atmosphere is probably drying out in the morning hours prior to the time significant convective activity can occur. Consequently, the model is being run with too much surface moisture, perhaps resulting in an overprediction of the convective activity for the day. On the days when the model underpredicted the activity (10 July and 13 July), there was a relative minimum in the precipitable water and surface moisture which was followed the next day by substantially increased precipitable water and

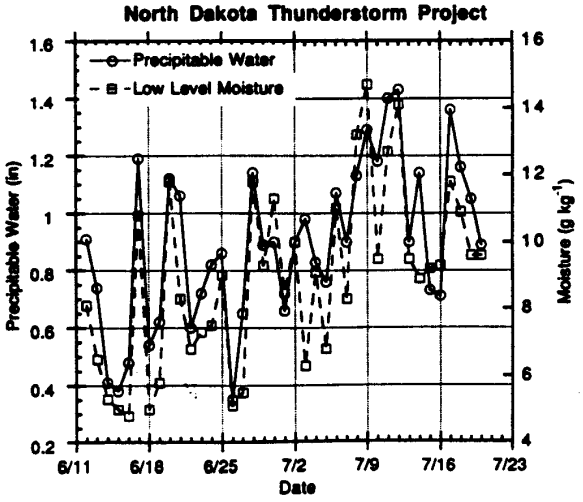

Fig. 6: Plot of precipitable water and low level moisture vs. the day of the project.

surface moisture, at least on the 10th. It may well have been during the day on the 10th that there was substantial advection of surface moisture into the region resulting in greater convective activity which was not picked up by the model as a result of the dryness in the 12 Z sounding.

5. CONCLUSIONS

The two-dimensional model was quite successful in simulating the convection on the basis of using the 12 Z sounding during the North Dakota project. It was able to do this in a predictive sense prior to the convection taking place. Results in a graphic form were available for a weather briefing in the late morning hours. While the model guidance was not used to any great extent by the project directors, there were times when they might have made better decisions if they had paid more attention to the model results. In particular, on one day the model forecast cloud tops to be at approximately the -2°C to -5°C level which would have been an ideal opportunity for a particular seeding experiment which was not conducted. This was nearly the only opportunity to have done so during the project.

Acknowledgments. This paper was written under sponsorship of the National Science Foundation under Grant No. ATM-8901355 and the National Aeronautics and Space Administration under Grant No. NAG-8-632. NOAA funding is also acknowledged under Contract No. ARB-IAS-89-2 with the North Dakota Atmospheric Resource Board. Thanks are also extended to Mrs. Joie Robinson for her work in preparing the manuscript.

REFERENCES

Orville, H. D., and F. J. Kopp, 1977: Numerical simulation of the life history of a hailstorm. J. Atmos. Sci., 34, 1596-1618. [Reply: J. Atmos. Sci., 35, 1554-1555]

APPENDIX C

Reprinted from the Preprint Volume of the 16th Conference on Severe Local Storms and the Conference on Atmospheric Electricity, October 22-26, 1990. Kananaskis Park, Alta., Canada. Published by the American Meteorological Society, Boston, Mass.

8.2

THE USE OF A CLOUD MODEL TO PREDICT CONVECTIVE AND STRATIFORM CLOUDS AND PRECIPITATION

Fred J. Kopp and Harold D. Orville

Institute of Atmospheric Sciences
South Dakota School of Mines and Technology
501 East St. Joseph Street
Rapid City, South Dakota 57701-3995

1. INTRODUCTION

The Institute of Atmospheric Sciences two-dimensional, time-dependent cloud model has been used on two field projects in the recent past to predict the characteristics of convection for the day. This means that the model was run from a morning sounding and various output attained to indicate to project personnel what the weather might look like on that day. Special graphic output was designed to show in a few frames the results of the simulation so that the field people could get an idea of what to expect. Normally, hundreds of frames of graphic output are needed for visualization of a simulation.

The two projects on which the test was run were COHMEX, conducted in the summer of 1986 in Huntsville, Alabama, and the North Dakota Thunderstorm Project run in 1989 in Bismarck, North Dakota. The output device planned to be used in COHMEX was not available at the last minute before the project started, so real time forecasts were not given during that project, although the model was run on the morning sounding before convection actually occurred and one case has been reported in Tuttle et al. (1989). However, in the North Dakota Project in Bismarck, the situation was such that model forecasts could be made every day and were a small addition to the amount of briefing material given by Howard Johnson, the forecaster on the project. One of us (FJK) actually made the model briefings.

The morning routine was for Fred Kopp to pick up the rawinsonde sounding at 0730 from the weather service. By 0815 or so, he would input temperature, the dew point and the winds, and send them to NCAR to initialize the model. By 0900, normally the integration was finished with only the more severe convective days taking more than the 40 min or so of CRAY XMP time. By 0915, the results would have been received from NCAR over a 9600 baud communications line. From 0930 to 1000, the data were copied and prepared for the briefing. Briefings were normally held at 1100, but every now and then on an early convection day, we would need to be ready by 1000.

2. MODEL DESCRIPTION

The theoretical framework is a deep-convection, two-dimensional, time-dependent cloud model which has been applied to a variety of atmospheric situations. A density weighted stream function has been used to extend the model to deep convection. Atmospheric wind, potential temperature, water vapor, cloud liquid, cloud ice, rain, snow, and graupel/hail (in the form of ice pellets, frozen rain, graupel, and small hail) are the main dependent variables. The nonlinear partial differential equations constituting the model include the first and third equations of motion, a thermodynamic equation, and water conservation equations (for its three phases). The model has been developed from the works of Orville (1965), Liu and Orville (1969), Wisner et al. (1972), Orville and Kopp (1977), and Lin et al. (1983).

The bulk-water microphysical scheme employed in the model is based on concepts suggested by Kessler (1969) and divides water and ice hydrometeors into five classes: cloud water, cloud ice, rain, snow, and high density precipitating ice (graupel/hail). These five classes of hydrometeors interact with each other and water vapor through a variety of crude parameterizations of the physical processes of condensation/evaporation, collision/coalescence and collision/aggregation, accretion, freezing, melting, and deposition/sublimation. Rain, snow, and graupel/hail, which are assumed to follow inverse exponential size distributions, possess appreciable terminal fall velocities. Cloud water and cloud ice have zero terminal velocities and thus travel with the air parcels. For a detailed discussion of the microphysical processes and parameterizations employed in the bulk water model, the reader is referred to Wisner et al. (1972), Orville and Kopp (1977), and Lin et al. (1983).

The model has been designed such that mesoscale convergence can be superimposed in the lower levels and divergence in the upper levels, which can result in stratus-type clouds being formed under certain atmospheric conditions. The manner in which mesoscale convergence is applied to the model and further details of the hydrodynamic equations can be found in Chen and Orville (1980).

Atmospheric sounding conditions of temperature, humidity, and wind are needed to initialize the model. Surface heating and evaporation rates may also be specified (as described in Liu and Orville, 1969). If information is available on larger scale convergence/divergence patterns, then these data can also be used in model runs.

The model uses a heat flux technique at the surface to warm the lower atmosphere and to eventually lead to convection. This method is taken from McNider and Kopp (1990) and has recently been described by Kopp et al. in the recent AMS Cloud Physics Conference (Kopp et al., 1990). At this date, a time changing heat flux has not been used, but only the average heat flux per day. Consequently, too much heat is added in the model early in the day and too little later on, which probably leads to convection earlier than might be expected. In the future, a time varying heat flux could be used to simulate the solar insolation being received at the earth's surface. Cloud shadow effects modulate the heat flux when clouds are formed. At this time, the average heat flux value is 300 W m^{-2}.

Evaporation is also simulated at the surface of the earth. In addition, if need be, moisture can be decreased in the lower atmosphere to simulate a drying condition occurring throughout the day which might be evident on the morning weather charts. Also, the morning weather charts indicate whether convergence or divergence should be simulated in the lower level with the opposite feature in the upper levels. This could also be an important feature for obtaining accurate predictions.

One other condition that is necessary for running this model is the ice initiation temperature. This temperature is crucial for the beginning of ice in the clouds and can mean the difference between a cloud forming precipitation or not because the clouds in the High Plains normally initiate precipitation through ice processes. Once precipitation has been formed in the cloud and snow is in the model anywhere, then subsequent precipitation formation can occur because of ingestion of ice particles. In only one or two cases did the clouds grow to a size such that the ice initiation temperature was critical. After a few days of being on the project, we settled on -18°C as being the ice initiation temperature and went throughout the rest of the season with that value.

3. MODEL RESULTS

The results from COHMEX have been presented by F. J. Kopp in the recent AMS Cloud Physics Conference. Results reported here will concentrate on the North Dakota Thunderstorm Project. The types of material available (not all were given in the briefings) are the horizontal averages versus height and time and the amount of rain that would fall or hail that would fall on the ground versus time. The variables that we had information on were the rain, graupel/hail, cloud water and cloud ice, and snow mixing ratios; the vertical velocity maximum, the surface temperature and the horizontal velocity at the surface; water vapor; the temperature throughout the atmosphere as well as at the surface; and some composite fields of these various variables. Examples of the results are given in Figs. 2 through 16.

Figure 1 is the atmospheric sounding for Bismarck at 12 Z on 28 June 1989. The figure shows a lifting index of about -5, precipitable water over one inch and a K index of 31, all indicating good potential for convection on this day. The winds were light from the east at 10 knots at the surface, increasing to 30 knots at 820 mb or so and 20 knots at 700 mb from the south, switching to the west at about 20 knots at 500 mb and above. It was agreed by all that this sounding was one in which you would expect deep convection, and that it would probably be severe.

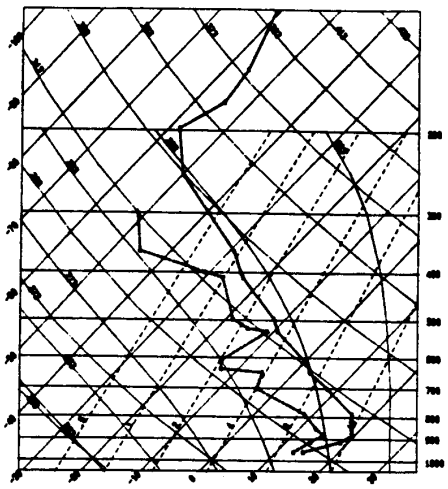

Fig. 1: Sounding for 1200Z on June 28, 1989 from Bismarck, ND, plotted on a skew T - log P diagram.

Figure 2 (28 June 1989) shows the cloud water and cloud ice content versus time. This graph shows when the cloud would form, the cloud base height, and what the cloud top would eventually grow to. The first cloud forms at about 240 min, four hours into the integration, and grows rather rapidly from a base at 2 km above ground level to nearly 14 km above ground level for the cloud top. These are horizontal averages of the water and cloud ice mixing ratios, so the largest values are not nearly as large as what actually occurred. The value "100" on these

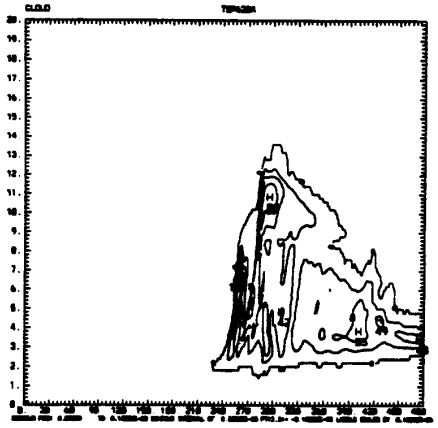

Fig. 2: Time-height contours of cloud substance. The abscissa is time in min and the ordinate is height in km. At each level in the model, the cloud water is averaged in the horizontal to get a point on the plot. Points are generated at 1-min intervals.

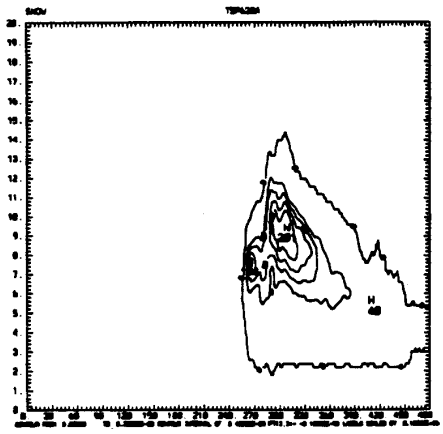

Fig. 3: As in Fig. 2, but for snow.

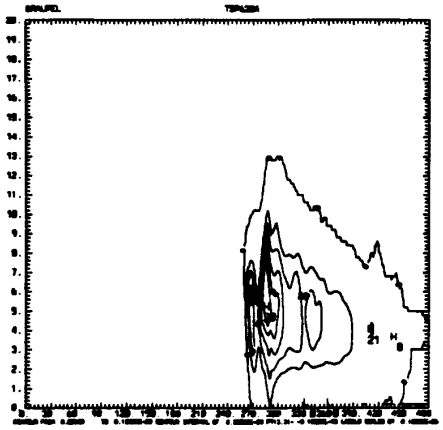

Fig. 4: As in Fig. 2, but for hail.

graphs stands for 1 g kg^{-1}. The cloud then decreases with time and becomes quite shallow by 480 min, or 8 hours of simulated real time.

Figure 3 shows the snow content, with snow first occurring between 7 and 8 km at about 260 min or so. Maximum values of 2 g kg^{-1} show up, but again realize that the horizontal average values are at 100 points summed up and divided by 100. Of course, this leads to a lot of zeroes being included and decreases the amount of water content significantly.

Figure 4 shows the graupel field with graupel first occurring about 270 min. Its source has been the snow field. Snow collects cloud water and aggregates to form graupel. There are two or three pulses in the graupel field. The graupel reaches a maximum value between 5 and 6 km above ground level.

Figure 5 shows the rain field, again occurring slightly after 270 min. Rain has formed from the melting of the graupel. The value "100" stands for 0.1 g kg^{-1}, so the maximum values here are around 0.8 g kg^{-1} of rainwater. The rain begins a little after 270 min and lasts throughout the rest of the integration period, but is decreased significantly after 450 min. A composite of the above fields is shown in Fig. 6.

Figure 7 shows the maximum vertical velocity versus time. This is not a horizontal average but the actual maximum vertical velocity that has occurred in the model domain versus height and time. The graph shows that a maximum value of 31 m s^{-1} was predicted by the model. This occurred as the cloud was reaching its maximum height, near 280 min of simulated real time.

Figure 8 shows the surface horizontal velocity versus time. The field is rather flat until the main convection has begun, and then around 280 min a very strong low level wind shear of 24 m s^{-1} differential in wind speed is detected. This shows the potential of the model for predicting microburst conditions.

Figure 9 shows the rainfall potential that was predicted for this day. This is not a horizontal average; the graph shows the amount of rain that has accumulated at the earth's surface. The maximum value of 3.77 cm was reasonable for this day.

Figure 10 shows the hailfall in the model with a value of a little over 1.2 cm. Since this is an accumulated amount of hail on the ground, the actual hailstone size would be nearly twice this size, assuming spherical hailstones (monodispersed and a single layer of stones).

Figure 11 shows the model's two-dimensional (x-z) output at 285 min, the time of maximum vertical velocity. It shows a rather severe storm topping out around 12 km. In Fig. 11, the cloud outline denotes the areas of greater than 100% relative humidity with S symbols indicating snow and the horizontal dashes within the cloud outline giving ice contents > 0.5 g kg^{-1}, the asterisks and the dots giving graupel/hail, and rain contents > 1 g kg^{-1}. The vertical velocities are shown in Fig. 12 with a maximum value of 31 m s^{-1}.

Figure 13 shows the horizontal position of clouds. Clouds show up at 240 min at 2 km in from the left boundary and 6 or 7 km in from the left boundary. Later on, clouds cover most of the grid. This figure is useful because it indicates whether or not the clouds are forming on the boundaries, which is of concern to modelers.

Figure 14 shows the surface temperature versus time. The maximum temperature changes rather steadily from around 16°C to > 32°C on this day and then when the clouds form the temperature falls.

Figure 15 shows a composite of the cloud, rain, hail, and snow fields; a result for this day with no surface evaporation. The maximum rain in this case was about 0.3 of a centimeter, only 10% as much as in the case with evaporation. Again, this shows the great importance of evaporation. Also note that the cloud top is only a little over 10 km.

Figures not shown are those for precipitable water (which showed values to 4 cm), temperature and water vapor throughout the atmosphere.

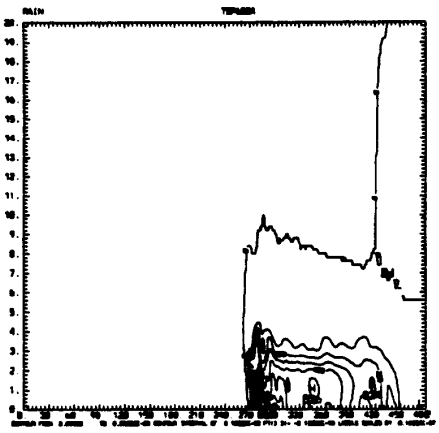

Fig. 5: As in Fig. 2, but for rain.

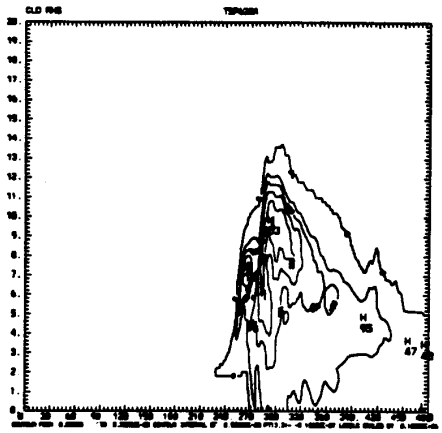

Fig. 6: As in Fig. 2, but the cloud, snow, graupel, and rain are added together.

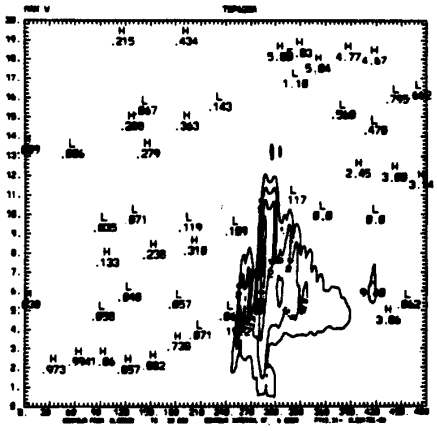

Fig. 7: As in Fig. 2, except that the maximum vertical velocity is plotted from each level.

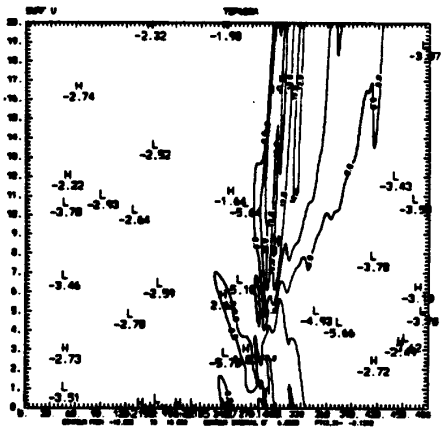

Fig. 8: The surface wind vs. time. The abscissa is time and the ordinate is distance from the left boundary of the model. At 1-min intervals, the horizontal velocity is plotted and contoured.

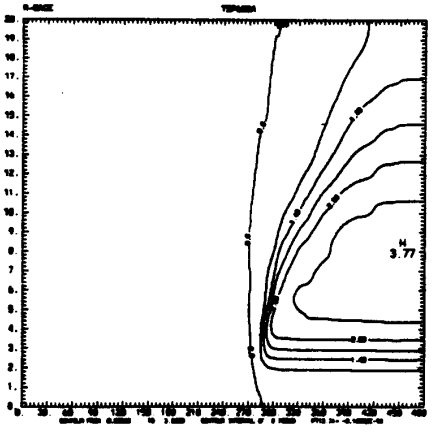

Fig. 9: Rain gage. The abscissa is time and the ordinate distance from left boundary. The depth is contoured in cm.

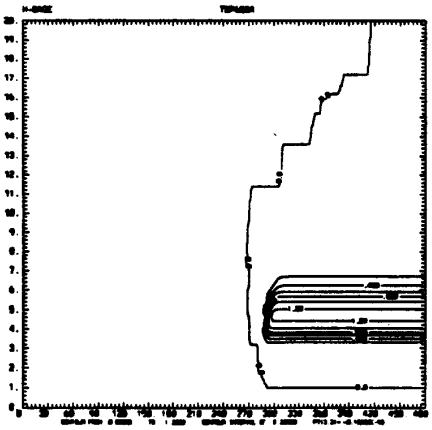

Fig. 10: Hail gage. See Fig. 9 for description of axis.

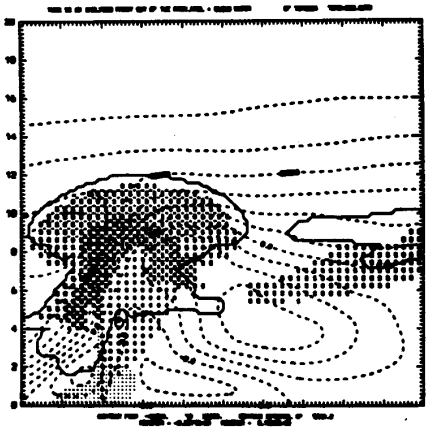

Fig. 11: Depiction of cloud and precipitation at 285 min. The abscissa and ordinate are distance. The cloud is outlined and rain, graupel, and snow are depicted by •, *, and S, respectively. The dashed lines are streamlines.

The weather on this day was violent; severe convection, tornadoes, and hail did occur. Cloud tops were greater than 13 km. There were also very strong gusts at the surface and updrafts in one cloud were measured to be 31 m s^{-1}. The University of Wyoming King Air encountered this strong updraft and had a very turbulent time in the cloud. The cloud development was extremely rapid, and most of the pilots complained about the severe conditions that they encountered. Rains of greater than one inch occurred in several places. An actual mesoscale convective system developed and spread over a good part of North Dakota before the day was over.

A case in which we actually missed a prediction is shown in Fig. 16. On this particular day, the predicted development was much greater than that which actually occurred. We suspect

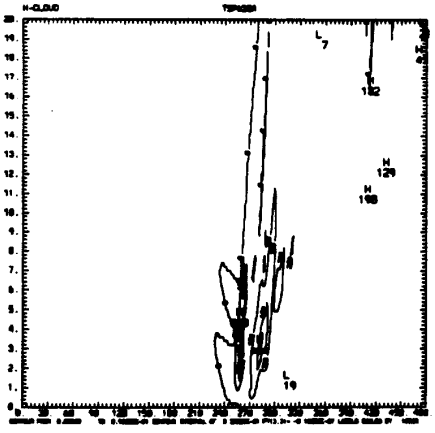

Fig. 13: Cloud position vs. time. The axes are as in Fig. 8. The contours are of the cloud summed in the vertical. The horizontal extent of the clouds are shown.

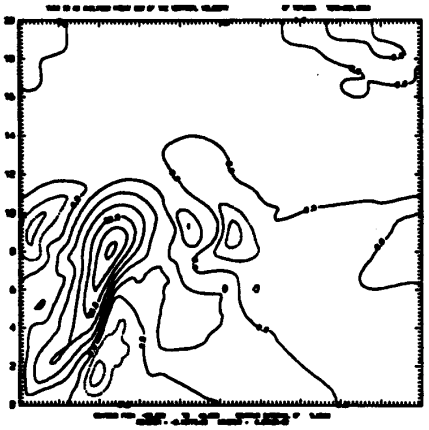

Fig. 12: Updraft at 285 min. The abscissa and ordinate are distance. Contour interval is 5 m/s.

that changes in the water vapor were very crucial for this situation.

We kept a qualitative account of whether or not the model seemed to be catching the main characteristics of the clouds for the day. Not all the time was convection, the main cloud forming process. The first few days of the project, low level clouds were formed by convergence, and stratiform clouds were the primary result. The model was able to simulate these clouds because of the convergence/divergence values which could be superimposed on the initial conditions. In general, we hit on about three out of four cases, 30 out of 40 cases that were predicted for this project.

Figure 17 shows the hits and the misses, as qualitatively determined during the project.

4. CONCLUSIONS

We conclude that some skill is shown by the model in predicting the characteristics of

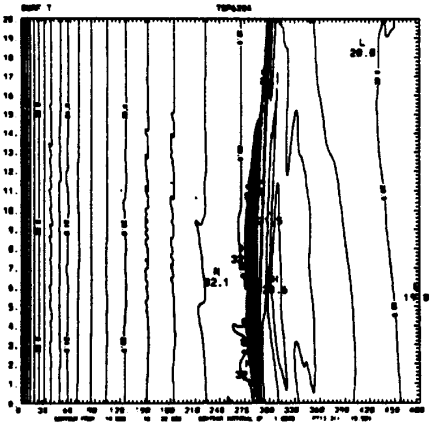

Fig. 14: As in Fig. 8, but for surface temperature.

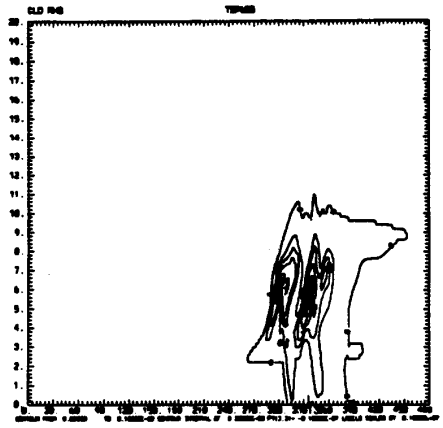

Fig. 15: As in Fig. 6, but for no evaporation case.

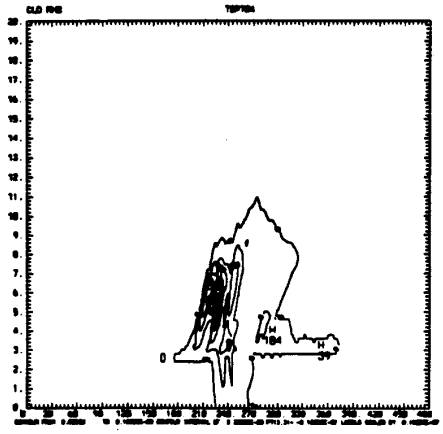

Fig. 16: As in Fig. 6, but for a case on July 4, 1989, which was overforecast by model.

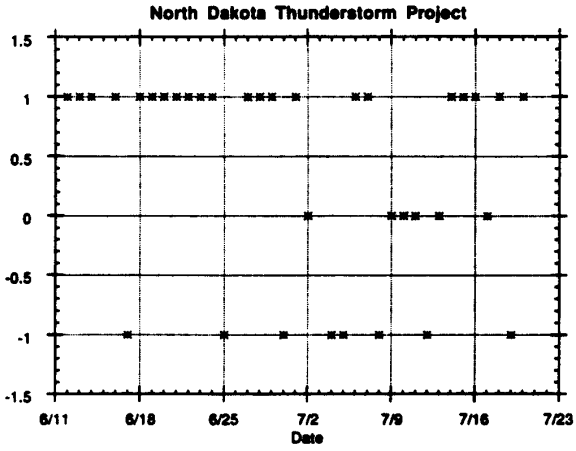

Fig. 17: Plot of hits and misses with model. Abscissa is month/day and ordinate is +1 for hit, 0 for partial success, and -1 for miss.

clouds on the various days throughout the summer project.

1) Overprediction was the primary miss when it did occur.

2) The initial conditions can be very important and are controlled by the modeler. In particular, whether or not you use superimposed convergence or divergence and what the water vapor changes would be can be very important to the results.

3) Surface boundary treatment is important. Heat and vapor fluxes from the surface can be crucial for the results. The heat flux method developed by McNider and Kopp (1990) works well.

4) Ice initiation temperatures can be crucial in marginal precipitation situations. In this part of the country, ice processes are crucial for precipitation and can determine whether or not rain will or will not fall from marginal size clouds.

In general, we were pleased with the results of the test and think that the field project personnel came to have some appreciation for model results throughout the period of the project. Certainly, improvements can be made which would make cloud models an even more important part of major field projects.

It also appears that the model could be used to predict low-level wind shears in critical situations.

Acknowledgments. This work has been supported by the National Science Foundation under Grant No. ATM-8901355 and by the North Dakota Atmospheric Resource Board under Contract No. ARB-IAS-89-2. Thanks are given to Joie Robinson and Sandra Palmer for typing this manuscript.

REFERENCES

Chen, C-H., and H. D. Orville, 1980: Effects of mesoscale convergence on cloud convection. J. Appl. Meteor., 19, 256-274.

Kessler, E., 1969: On the distribution and continuity of water substance in atmospheric circulations. Meteor. Monogr., 10, 32. 84 pp.

Kopp, F. J., H. D. Orville, J. A. Jung and R. T. McNider, 1990: A parameterization of radiation heating at the surface in a numerical cloud model. Preprints Conf. Cloud Physics, 23-27 Jul 1990, San Francisco, CA, Amer. Meteor. Soc., —.

Lin, Y-L., R. D. Farley and H. D. Orville, 1983: Bulk parameterization of the snow field in a cloud model. J. Climate Appl. Meteor., 22, 1065-1092.

Liu, J. Y., and H. D. Orville, 1969: Numerical modeling of precipitation and cloud shadow effects on mountain-induced cumuli. J. Atmos. Sci., 26, 1283-1298.

McNider, T. R., and F. J. Kopp, 1990: Specification of the scale and magnitude of thermals used to initiate convection in cloud models. J. Appl. Meteor., 29, 99-104.

Orville, H. D., 1965: A numerical study of the initiation of cumulus clouds over mountainous terrain. J. Atmos. Sci., 22, 684-699.

Orville, H. D., and F. J. Kopp, 1977: Numerical simulation of the life history of a hailstorm. J. Atmos. Sci., 34, 1596-1618. [Reply: J. Atmos. Sci., 35, 1554-1555]

Tuttle, J. D., V. N. Bringi, H. D. Orville and F. J. Kopp, 1989: Multiparameter radar study of a microburst: Comparison with model results. J. Atmos. Sci., 46, 601-620.

Wisner, C. E., H. D. Orville and C. G. Myers, 1972: A numerical model of a hail-bearing cloud. J. Atmos. Sci., 29, 1160-1181.

APPENDIX D

OBSERVATIONS AND MODEL SIMULATIONS OF TRANSPORT AND PRECIPITATION DEVELOPMENT IN A SEEDED CUMULUS CONGESTUS CLOUD

Michael W. Huston,[1] Andrew G. Detwiler and Fred J. Kopp

Institute of Atmospheric Sciences
South Dakota School of Mines and Technology
501 East St. Joseph Street
Rapid City, South Dakota 57701-3995

and

Jeffrey L. Stith

Department of Atmospheric Sciences
University of North Dakota
Box 8216 University Station
Grand Forks, North Dakota 58202

---

[1]Present Address: 726 Long Drive, #14A, Sheridan, WY 82801.

ABSTRACT

Observations made by three instrumented aircraft, a Doppler radar, and other data sources were used to follow the initiation and development of precipitation in a small cumulus congestus cloud. The cloud was seeded at its base using an airborne silver iodide solution burner. Sulfur hexafluoride tracer gas was released along with the seeding material. Analyzers on two instrumented aircraft detected the tracer gas during subsequent cloud penetrations as it was carried up into the cloud along with the seeding agent. Ice developed initially in the upper regions of the cloud near the -10°C level ~15 minutes after the commencement of seeding. This is consistent with primary nucleation by the seeding agent. The cloud developed millimeter-sized graupel within the following few minutes. A radar echo approaching 40 dBz subsequently developed. The echo was observed to descend through the cloud as the cloud dissipated.

A one-dimensional, steady-state and a two-dimensional, time-dependent, bulk water model were used to simulate this cloud. The one-dimensional model produced realistic values for updraft speeds allowing credible estimates of time required for transport from cloud base to upper regions of the cloud. The development of precipitation in the two-dimensional simulation resembled that in the observed cloud. Precipitation developed through riming of snow to graupel. In both the observed and simulated clouds, precipitation development was limited by cloud lifetime. Both clouds collapsed at a

time when they were still generating ample supercooled water in their updrafts. Total precipitation on the ground from the seeded cloud simulations was ~ 5X the radar estimated rainfall total of 0.5 mm from the observed seeded cloud. This occurred despite the fact that the simulated cloud went through an accelerated life cycle compared to the observed cloud. A comparison between simulations with a natural ice process and with cloud base release of silver iodide shows that seeding accelerated precipitation formation in the model cloud leading to a 4X increase in total precipitation for the seeded cases compared to the natural one.

APPENDIX E

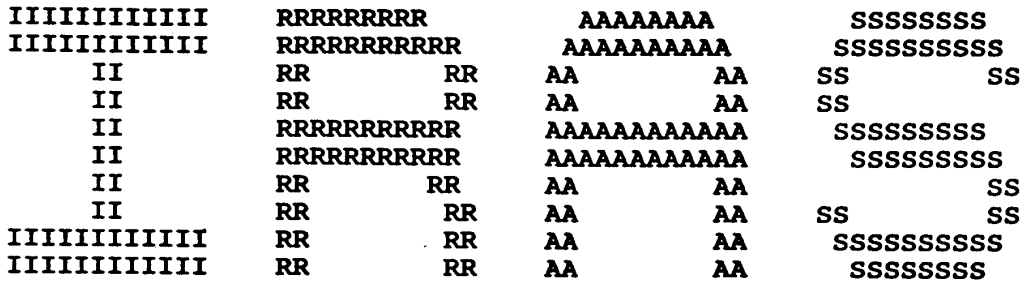

Interactive Radar Analysis Software

User's Guide

Version 1.0

February 14, 1990

About this Manual

This document describes how to use the Interactive Radar Analysis Software package (IRAS). It was developed at the Institute of Atmospheric Sciences to support radar data analyses for several research programs. Support was initially provided under a contract from the North Dakota Atmospheric Resource Board for analysis of Chill weather radar data collected at Dickinson, North Dakota during the summer of 1987. However, as this software package evolved, it was determined that it would be usefull to researchers involved in the analysis of weather radar data collected from other research projects. Therefore, additional support was provided under these programs to expand the capabilities of IRAS.

Using this Manual

This manual has been divided into 4 chapters. Chapter 1 contains a brief introduction to IRAS. Chapter 2 describes how to configure your system before running IRAS. Chapter 3 details the required format of the radar data used by IRAS. Chapter 4 describes how to use IRAS and provides detailed explanations about the options which are avaibable.

Conventions Used in this Manual

Several conventions have been used while preparing this document. The symbol "->" is used for the DOS prompt and "$" for the VAX prompt. Items enclosed in brackets "()" indicate user supplied information. Commands are all capitalized along with any reference to specific keyboard keys.

Additional Comments

If anyone has any questions regarding the contents of this document, contact the following individual:

David L. Priegnitz
Institute of Atmospheric Sciences
South Dakota School of Mines & Technology
Rapid City, SD 57701
(605)-394-1993

APPENDIX F

Reprinted from the Preprint Volume of the Eighth Conference on Hydrometeorology, October 22-26, 1990, Kananaskis Park, Alta., Canada. Published by the American Meteorological Society, Boston, Mass.

7.1

ESTIMATION OF CONVECTIVE RAIN VOLUMES UTILIZING THE AREA-TIME-INTEGRAL TECHNIQUE

L. Ronald Johnson and Paul L. Smith

Institute of Atmospheric Sciences
South Dakota School of Mines and Technology
501 East St. Joseph Street
Rapid City, South Dakota 57701-3995

1. INTRODUCTION

Interest in the possibility of developing useful estimates of convective rainfall with Area-Time Integral (ATI) methods is increasing (Smith et al., 1990; Atlas et al., 1990). In practice, the rainfall volume V from a convective system over a time interval can be identified as:

$$V = \bar{R} \sum_i A_i \, \Delta t_i \quad . \qquad (1)$$

Here A_i represents the area over which some measured quantity exceeds a specified threshold during the (centered) time interval Δt_i between observations. The measured quantity can be gage rainfall rate, but radar reflectivity factor or satellite infrared temperature can also be used. The summation extends over the duration $T = \sum \Delta t_i$ of the rainfall event of interest. The quantity $\bar{R}$ represents the average rainfall rate over the identified area for the case under study. The summation in (1) is identified as the ATI.

The basis of the ATI technique is the observed strong correlation between rainfall volumes and ATI values. This means that rainfall can be estimated by just determining the ATI values, if previous knowledge of the relationship to rain volume is available to calibrate the technique. The ATI's can be determined from rain gage data, if the gage density and time resolution are sufficient (Doneaud et al., 1979, 1981); from radar data (Doneaud et al., 1981, 1984; Lopez et al., 1989); or from satellite infrared observations (Doneaud et al., 1987; Smith et al., 1990). The respective thresholds involve the minimum measurable amount of rainfall, a minimum radar reflectivity factor, or a maximum IR brightness temperature. Correlations found between ATI values determined from any of these sources and rainfall amounts determined either from gages or radar data have been 0.9 or greater in every case studied thus far. For radar ATI's in particular, the correlation is typically 0.98.

This paper provides examples of the application of the ATI approach to gage, radar, and satellite measurements. For radar data, the degree of transferability in time and among geographical areas is examined. Recent results on transferability of the satellite ATI calculations will be presented at the conference.

2. APPLICATION TO RAIN GAGE DATA

With a dense network of recording gages, ATI values can be calculated from (1) by considering each gage that receives a threshold amount of rain during the specified time interval. The area A_i can be established using a method such as Thiessen polygons. A rough estimate of the ATI can be obtained by assuming each gage to represent an equal area, if the network is not too far from uniform.

Such an analysis was made for McKenzie County, North Dakota, in the summer of 1972 (Doneaud et al., 1979). There were 22 recording gages distributed over an area of 7374 km^2, and the readings were reduced to hourly data which were used to obtain the gage ATI values. The results were compared with estimates of 12-hr rainfall over the area obtained from a separate network of 65 non-recording gages (read twice daily) over the same area. Figure 1 shows the results of this comparison for the 18 rain days having at least 3 gage-hours of recorded data. (The synoptic classification in the figure is not of concern here.)

The slope on this log-log plot is about 1.16. It was recognized that even 65 gages might not give a good estimate of the areal rainfall, especially for the smaller events, so a similar analysis was done using radar to estimate the area rainfall. That analysis yielded a slope of about 1.03 (agreeing better with those in Table 1 below).

To place an absolute scale on the abscissa, note that 1% of the possible gage-hour rain events ($x = 0.0$ in Fig. 1) would correspond to an ATI of about 885 km^2·hr. On the ordinate in the figure, $y = 0.0$ corresponds to a rain volume of 10^3 kt = 10^3 km^2·mm. The regression lines for the gage and the radar estimates of the area rainfall would intersect at about $x = 1.0$ (ATI = 8850 km^2·hr), $y = 1.5$ (rain volume = 3.16×10^4 km^2·mm); at that point, the average rainfall rate over the rainy area would be 3.6 mm hr^{-1}. This compares favorably with the average rates obtained using a reflectivity threshold of 25 dBz to calculate the ATI from radar data. This fact suggested that we were on the right track, even though much concern has recently been expressed about the selection of the proper threshold (Atlas et al., 1990).

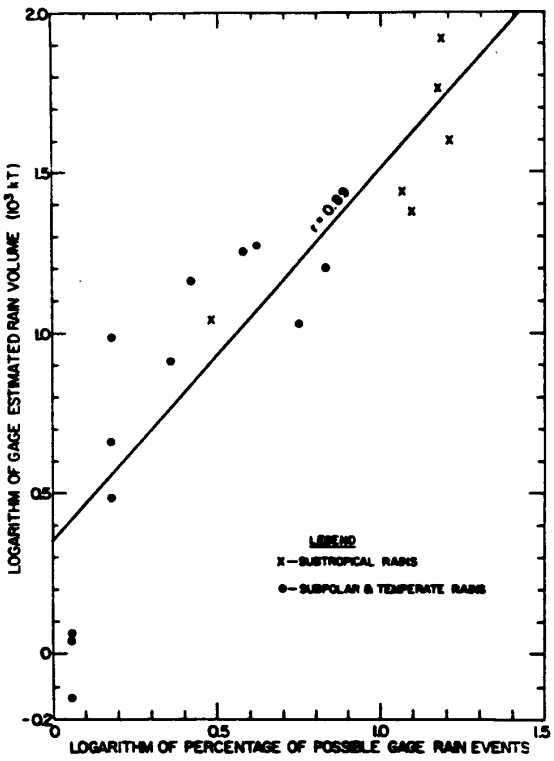

Fig. 1: Log-log plot of gage-estimated daily rain volume for McKenzie County, North Dakota vs. the percentage of possible gage-hours which actually had rain. The abscissa can be converted into an ATI as indicated in the text.

3. APPLICATION TO RADAR DATA

The most extensive uses of the ATI concept to date have involved radar observations. For example, during the Cooperative Convective Precipitation Experiment (CCOPE) that occurred in 1981 in southeastern Montana, radar volume-scan data were recorded continually during declared "go" days by a C-band radar system with 1° beamwidth. An extensive study of the CCOPE radar echo clusters was accomplished (Johnson and Hjelmfelt, 1990). Since the life history of each cluster was known, calculation of the Area-Time Integrals for these clusters was straightforward. Calculation of rainfall amounts using a Z-R relationship developed for the region ($Z = 155\ R^{1.8}$, Smith et al., 1975) was accomplished at the same time.

Figure 2 compares the resultant radar-estimated rainfall to the Area-Time Integral for 865 clusters for which time histories are available. The log-log plot indicates extremely good correlation over a range that exceeds five orders of magnitude in rainfall. Regression analysis demonstrates a correlation coefficient of 0.988, with y-intercept of 0.326 log (km² mm) and slope of 1.088. The root-mean-square logarithmic error of 0.145 translates to a factor 1.4. Given any radar ATI that is computed using the same reflectivity threshold of 25 dBz, a straightforward rainfall estimate can be produced using Fig. 2.

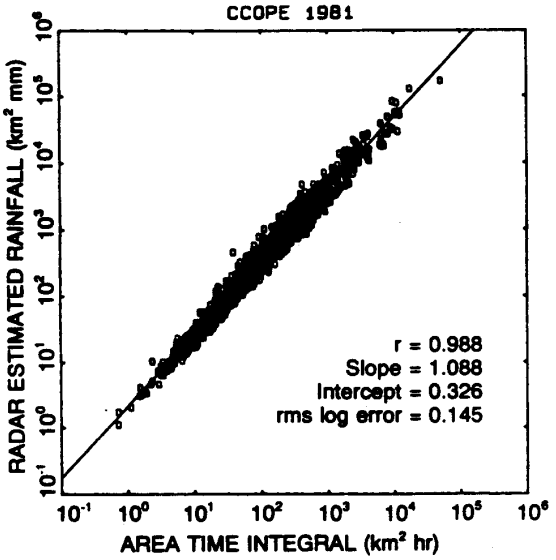

Fig. 2: Log-log scatter plot of ATI vs. radar estimated rain volume for echo clusters from CCOPE. Solid line shows the regression result.

Such comparison of area-time integral values to radar-estimated rain volumes using an appropriate Z-R relationship has been accomplished for several projects; the results are presented in Table 1. Each regression relationship like that established in Fig. 2 results in a power-law relation of the form

$$V = K \times ATI^{b} \quad , \qquad (2)$$

where V is rain volume; K and b are constants determined by regression. Specifically, b is the slope and K is the antilog of the intercept.

TABLE 1

ATI-Radar Rainfall Parameters Determined by Regression for Several Projects and Different Radars

PROJECT (YEAR)	K	b	RADAR (Type, Beamwidth)
NDPP (1972)	2.62	1.09	S-band, 2°
NDCMP (1980)	3.68	1.01	C-band, 2°
NDCMP (1981)	3.07	1.08	C-band, 2°
NDCMP (1982)	3.74	1.02	C-band, 2°
NDCMP (1984)	3.57	1.03	C-band, 2°
CCOPE (1981)	2.12	1.09	C-band, 1°
FACE (78, 79, 80)	3.40*	1.00	S-band, 2°
COHMEX (1986)	6.01	1.05	S-band, 2°

*18-dBz threshold used for ATI.

The first six entries of the table are for data from the western portion of North Dakota and eastern Montana, which represent similar geographic locations. For those six entries, the b parameter varies only from 1.01 to 1.09, while the K parameter varies from a low of 2.12 for CCOPE to a maximum of 3.74. Thus, we see small year-to-year variations as well as some differences (especially in K between Montana and North Dakota in the same year, 1981) that may be partly due to differences in radar characteristics.

The COHMEX data from the southeastern U.S. have a similar b parameter but the K parameter is substantially larger. This increase may be a climatological difference or only an artifact of the data. The WSR-57 RADAP data for COHMEX were recorded out to ranges of 250 km versus only 150 km for the ND/MT data. At ranges >150 km, with a 2° beamwidth, the sampling volume becomes rather large. Using the criterion that the reflectivity factor for the sampling volume has to exceed 25 dBz requires that a significant storm event must be taking place at the larger ranges before its inclusion in this study. Therefore, the larger coefficient may simply reflect greater rain amounts from these more mature events.

On the other hand, a similar radar was used in southern Florida during the FACE project for 1978, 1979, and 1980. Lopez et al. (1989) presented a composite figure for the three years comparing integrated radar echo area to radar-estimated rain volume. Their figure is similar to Fig. 2 except that linear scales were used. Scatter was evident about a line of slope 1 (which would have the same slope on a log-log plot); parameter K for 1-hr integration steps at a threshold of only 18 dBz is the reported average rain rate of 3.4 mm hr^{-1}. This value compares rather well with the K values from the High Plains observations with 2° beamwidths, but raising the threshold to 25 dBz would yield a higher value. The instrumented region of the project was within 170 km range of the radar.

Transferability of these relationships can be tested by using one relationship (like Fig. 2) to estimate rainfall amounts for other data sets. For example, during the 1984 North Dakota Cloud Modification Project, echo clusters were determined as in the CCOPE study. For each cluster, the same Z-R relationship was used to produce an estimate of rainfall. In Fig. 3, these estimates are compared to rainfall amounts estimated by using the observed ATI values with the CCOPE relationship presented in Fig. 2. Here we are comparing 1984 radar data to an ATI-rain volume relationship determined from 1981 data obtained with a different radar beamwidth. Yet, Fig. 3 demonstrates that the two different estimation schemes are similar. The ATI-estimated rainfall amounts do tend to be lower than those obtained from the Z-R relationship. This is consistent with the lower K parameter for the CCOPE relationship, as indicated in Table 1.

In another attempt to determine geographical transferability of the ATI relationships, the data secured by the RADAP system at Nashville, Tennessee, during the COHMEX project were similarly analyzed. The results are demonstrated in Fig. 4. Again, the ATI-estimated amounts tend to be lower than those obtained using a Z-R relationship developed specifically for the project (Peterson et al., 1990). The scatter is larger than that seen for North Dakota in the previous figure, and the degree of underestimate is a little greater. That is also consistent with the differences in the K values in Table 1.

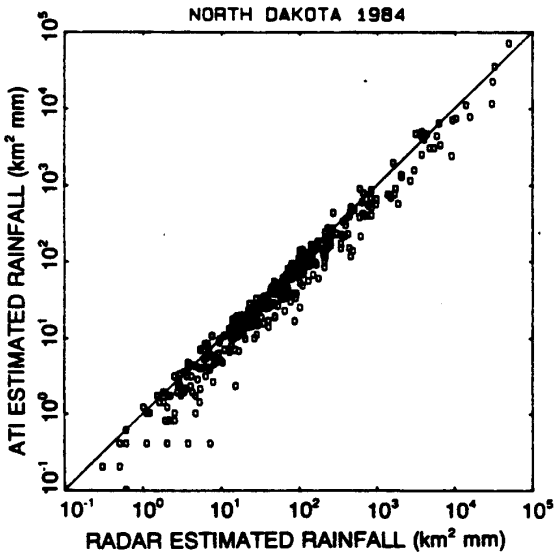

Fig. 3: Log-log scatter plot of rain volumes determined from the radar ATI using the CCOPE relationship (Fig. 2) for echo clusters from North Dakota 1984 vs. their direct radar-estimated rain volumes. The ideal 1:1 comparison line is shown.

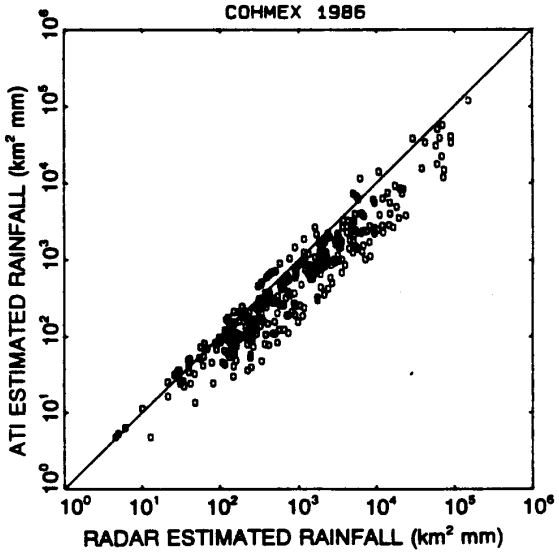

Fig. 4: Log-log scatter plot of rain volumes determined from the radar ATI using the CCOPE relationship (Fig. 2) for echo clusters from COHMEX 1986 vs. their direct radar-estimated rain volumes. The solid line shows the ideal 1:1 correspondence.

We cannot resolve the transferability question, with the data analyzed thus far. Using the same radar in the same location gives repeatable results (e.g., Doneaud et al., 1984). All our geographical comparisons also involve other differences, in wavelength, beamwidth, or range coverage. Thus we are not yet certain which are the more important factors, or whether they outweigh geographic differences.

4. APPLICATION TO SATELLITE INFRARED DATA

A special study with the major goal of establishing a satellite ATI method that could be used to estimate rain volumes is in progress. The initial analysis used radar data from the CCOPE and North Dakota-81 field projects as ground truth for comparison to satellite infrared rapidscan data. By optimization, it was determined that the ATI calculated using the area enclosed by the -23°C isotherm was most closely correlated to the radar-estimated rainfall. The results are presented in Fig. 5 and are discussed in Smith et al. (1990).

This satellite-identified ATI is significantly different from the ATI determined by radar or rain gages. The satellite ATI does not represent just the rainy portion of the storm, but, in fact, is many times greater. The slope in Fig. 5 is substantially less than unity, indicating that the satellite ATI grows more rapidly than the corresponding rain volume. Yet the optimization shows the area enclosed by the -23°C isotherm to be most closely related to the rain volume. Thus we expect to obtain good estimates of storm rain volumes, although accurate positioning of the rainfall on the surface will not be possible.

5. CONCLUSIONS

Application of the Area-Time Integral technique to estimate rain volume is very successful with comparable radar data. The same correlations appear in gage data where the gage network is sufficiently dense. The technique also appears promising using satellite infrared data.

Still, many questions need to be answered. It is obvious that a radar-determined relationship for the northern Great Plains may not be applicable to the more moist environments of the southeastern United States. Signs of such differences appear in our results, but other equipment or analysis variations muddy the picture at this time. We need more direct comparisons with similar radars in different geographic areas to resolve the transferability issue.

Using satellite data requires better identification of rain-producing events before application of the ATI method. The satellite ATI calculation does not insure a raining event, but can reasonably estimate the amount of rainfall given that rain is occurring. We need more extensive testing of the method with satellite data to determine how to circumvent this concern as well as to investigate geographic transferability.

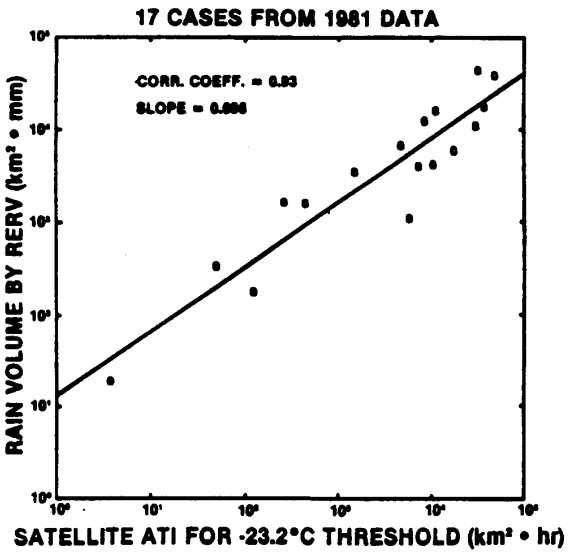

Fig. 5: Scatter plot and linear regression of cloud cluster rain volume (estimated by radar) vs. satellite ATI, for the optimized infrared threshold temperature of -23°C.

Acknowledgments. This research was sponsored by the North Dakota Atmospheric Research Board under Contract No. ARB-IAS-89-2 and the National Aeronautics and Space Administration under Grant No. NAG 5-386.

REFERENCES

Atlas, D., D. Rosenfeld and D. A Short, 1990: The estimation of convective rainfall by area integrals, 1, the theoretical and empirical basis. J. Geophys. Res., 95, 2153-2160.

Doneaud, A. A., S. Sengupta, P. L. Smith, Jr., and A. S. Dennis, 1979: A combined synoptic and statistical method for forecasting daily rain volume over small areas. Preprints 6th Conf. Probability and Statistics in Atmos. Sci., Banff, Alberta, Canada, Amer. Meteor. Soc., 39-45.

Doneaud, A. A., P. L. Smith, A. S. Dennis and S. Sengupta, 1981: A simple method for estimating convective rain volume over an area. Water Resources Res., 17, 6, 1676-1682.

Doneaud, A. A., S. Ionescu-Niscov, D. L. Priegnitz and P. L. Smith, 1984: The area-time-integral as an indicator for convective rain volumes. J. Climate Appl. Meteor., 23, 555-561.

Doneaud, A. A., J. R. Miller, Jr., L. R. Johnson, T. H. Vonder Haar and P. Laybe, 1987: The area-time-integral technique to estimate convective rain volumes over areas applied to satellite data - A preliminary investigation. J. Climate Appl. Meteor., 26, 156-169.

Johnson, L. R., and M. R. Hjelmfelt, 1990: A climatology of radar echo clusters over southeastern Montana. J. Wea. Modif., 22, 49-57.

Lopez, R. E., D. Atlas, D. Rosenfeld, J. L. Thomas, D. O. Blanchard and R. L. Holle, 1989: Estimation of areal rainfall using the radar echo area-time-integral. J. Appl. Meteor., 28, 1162-1175.

Peterson, B. A., D. J. Musil and P. L. Smith, 1990: Computerized reduction of airborne foil impactor data from COHMEX thunderstorms. Preprints Conf. Cloud Physics, 23-27 Jul 1990, San Francisco, CA, Amer. Meteor. Soc.

Smith, P. L., Jr., D. E. Cain and A. S. Dennis, 1975: Derivation of an R-Z relationship by computer optimization and its use in measuring daily areal rainfall. Preprints 16th Radar Meteor. Conf., Houston, TX, Amer. Meteor. Soc., 461-466.

Smith, P. L., L. R. Johnson, T. H. Vonder Haar and Don Reinke, 1990: Radar and satellite area techniques for estimating convective precipitation. Preprints Conf. Operational Precipitation Estimation and Prediction, Anaheim, CA, Amer. Meteor. Soc., 32-35.

APPENDIX G

A STUDY OF RADAR ECHO CLUSTERS OVER SOUTHEASTERN MONTANA

L. Ronald Johnson and Mark R. Hjelmfelt
Institute of Atmospheric Sciences
South Dakota School of Mines and Technology
501 East St. Joseph Street
Rapid City, South Dakota 57701-3995

Abstract. Data recorded by the Skywater radar during the Cooperative Convective Precipitation Experiment were used to produce echo cluster statistics. The average echo cluster is initiated in the mid-afternoon (15:18 MDT) and continues for 1.8 hours. It has a maximum reflectivity of 45.4 dBz, and produces 296 $km^2 \cdot mm$ of rainfall. The storm moves from the west to east at a speed of 12.5 m/s. Analysis revealed a bimodal distribution of maximum echo heights with the low mode at 6.9 km and the upper mode at 9.4 km. Comparison of predictors for radar estimated rainfall confirmed the value of the Area-Time-Integral (ATI). Echo statistics were in good agreement with those obtained from a different project in North Dakota for the same year, with greater differences obtained for statistics from projects in more humid climates. The importance of year-to-year variability is affirmed.

1. INTRODUCTION

During the course of the 1981 Cooperative Convective Precipitation Experiment (CCOPE) centered at Miles City, Montana, a wealth of data was accumulated by many investigators interested in precipitation-producing convective weather systems and beneficial modification of those systems. From these data, many studies have been conducted. Reports have included case studies, moisture budgets, and time histories (Fankhauser et al., 1985; Dye et al., 1986; Koch et al., 1988; Knight and Knupp, 1986; Miller et al., 1988; Rasmussen and Heymsfield, 1987; and Schmidt and Cotton, 1989). Beyond the case studies of particular events that occurred during the field season, few investigators have studied statistical aspects of echo clusters utilizing the existing radar data. This study was accomplished to prepare a composite description of the echo clusters observed in CCOPE. Such a composite should be useful in the comparison of southeastern Montana convective climatology to that of other areas, and to provide a useful data base. Consideration of these results in the design of future weather modification projects for the region should prove beneficial.

The results of the present study can be placed in a broader geographical context by comparison with similar studies performed in other parts of the country. Smith et al. (1985) presented a study of radar echoes observed in western North Dakota during the summers of 1981 and 1982 as a part of the North Dakota Cloud Modification Project. Their results provide a basis for comparisons with nearby data during the CCOPE season and also provide information on year-to-year variability. The motion of radar echo clusters over the Black Hills of South Dakota was studied by Kuo and Orville (1973). Dennis et al. (1971) reported on radar observations of hailstorms in western Nebraska. Foote et al. (1979) presented data on radar cells observed in the National Hail Research Experiment (NHRE) in northeast Colorado, southeast Wyoming, and western Nebraska. These two studies provide comparisons for intense storms further south in the High Plains. Huff (1987) statistically analyzed data collected on radar storm echoes in Illinois. This study is especially interesting as it provides a contrast between storms observed in the northern Great Plains with those in the more moist Midwest. His study was directed to applications to weather modification, and we will draw upon his results at several points in our discussion.

Results of data collected near St. Louis during the Metropolitan Meteorological Experiment (METROMEX) are summarized in Braham (1981). This study provides results on a slightly different population at the southern edge of the area covered in Huff's (1987) study. Lopez et al. (1984) stratified data on Florida rainstorms in several different categories. Some statistics of storms of similar lifetimes to those observed in the present study are presented.

2. DATA SOURCE AND PROCESSING

For this study, all volume scans recorded by the Skywater radar located near the Miles City airport during CCOPE were acquired. The data set begins with 20 May and continues through 6 August. A typical data recording day started at 1000 local time (all times given are local daylight time) and continued as long as echoes were present or until 2300, whichever occurred first. On 17 July, recording started at 0900; this first hour of collected data is intentionally left out of studies based on time of day.

The Skywater radar operated at a frequency of 5.55 GHz, a pulse repetition frequency of 414 Hz, and a pulse duration of 2 μsec with a horizontal beamwidth of 0.9° and a vertical beamwidth of 1°. The radar was located at latitude 46:24:46 north and longitude 105:55:13 west at an altitude of 802.6 MSL. The data bin width along the radial was one-half kilometer. In the volume scan mode, the first complete azimuth scan covered one rotation in 1° azimuth steps at 1° elevation.

The elevation was then increased in 1° increments to a maximum of 12° with a complete rotation at each elevation step. The volume scans were repeated at approximately 5-minute intervals. The data were provided by the U.S. Bureau of Reclamation in the A-file format (Schroeder and Klazura, 1978). A software procedure applied the calibrations that accompanied the requested tapes and compressed the resulting data into reflectivity files. Compression included removal of blue sky and other regions with echoes less than the threshold value (typically 6 dBz). The compressed reflectivity or "dBz" files were used for all succeeding processing.

The first product derived from the dBz file was a CAPPI-like product called "low tilt." It combines the 3° elevation scan from 20-50 km range with the 1° elevation scan for ranges beyond 50 km. Data within a 20 km radius of the radar site were eliminated to minimize ground clutter effects. Data beyond 200 km were also eliminated for the purpose of minimizing range effects. Using the low-tilt product from each volume scan, an echo cluster was defined as one or more contiguous bins with echo meeting the criteria indicated in the next paragraph. The identified cloud cluster commenced at the earliest scan time possible and was followed until dissipation. The cluster was "boxed" by defining range and azimuth coordinates for box corners that enclosed the cluster. The boxing information is used as input into another software utility which derives specific parameters related to volume and area as illustrated in Table 1.

Clusters were chosen when they met specific criteria: 1) the cluster had to be present during four consecutive scans, or exist for at least 30 minutes; 2) maximum reflectivities had to equal or exceed 25 dBz; 3) the cluster lifetime had to be contained within the radar surveillance area; and 4) if the cluster passed over the 20 km blanked area around the radar during its lifetime, it was dropped from further consideration. Echo splits occurred occasionally in the data set and, when they did, the original cluster identification was maintained for that portion of the echo that continued on the path nearest that of the original cluster. This portion usually exhibited the larger echo area. A new cluster designation was established for the other portion derived from the split if it continued as an entity for the required 30 minutes with reflectivities > 25 dBz. In the event that a small portion split from the main cluster and subsequently decayed within the 30-minute time frame, this portion was included as part of the original cluster. Echo mergers occurred as well; the dominant cluster involved in the merger was considered as the continuing cluster, with the other merging cluster's lifetime ending at the time of merger.

Clusters which drifted into the radar surveillance area as a mature or decaying event were eliminated from the data set. Clusters with initial echo locations at the outer range limit of surveillance were eliminated. Figure 1 shows a slight depression in the number of clusters at maximum range due to this correction. The final data set consisted of 765 clusters.

A broad spectrum of echo size is represented by the studied clusters which range from isolated, one-cell events to multicellular events as large as mesoscale convective systems. No attempt was made to subdivide the cluster set by synoptic type or evolution characteristic such as line, area, or isolated echo. Huff (1987) found little evidence

TABLE 1

Parameters Defined from Each Cluster Lifetime

PARAMETER	DESCRIPTION
ID	A two character code assigned uniquely each day to identified clusters.
Time	Time of initial scan of the cluster.
Month, Day	Date of initial scan.
DOY	Day of year
Average Reflectivity	Average of the maximum reflectivity of each scan over the cluster's lifetime.
Average Height	Average of the maximum height of each scan over the cluster's lifetime.
Maximun Reflectivity	Maximum reflectivity for the cluster lifetime.
Maximum Height	Maximum height reached by the cluster during its lifetime.
ATI	Area-Time-Integral
Duration	Time difference between initial and final scan.
RERV	Radar estimated rain volume as computed by Z-R relationship.
Range	Average cluster distance from the radar for its lifetime.
Initial Range Initial Azimuth	Coordinates of the cluster first echo.
Surface 850 mb 700 mb 500 mb	Wind direction determined from the nearest sounding in space and time for the indicated levels.

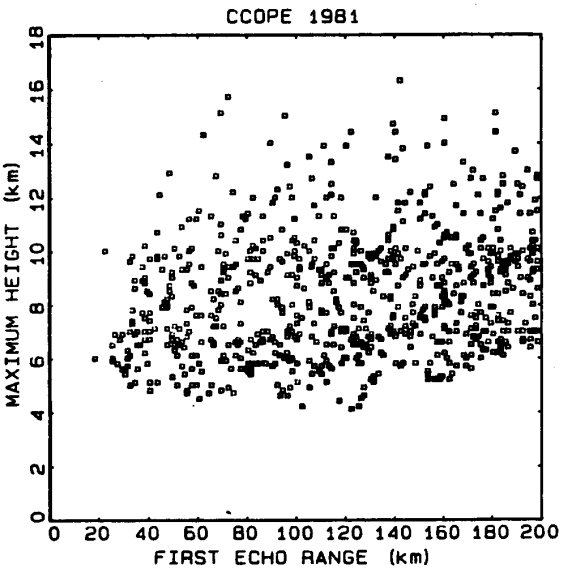

Fig. 1: Scatter plot of cluster lifetime maximum echo height as a function of first echo range (r = 0.22, slope = 0.010).

to distinguish differences by synoptic type for radar echoes studied from Illinois. A large portion of the CCOPE echoes either had their initiation in a line formation or their initiation helped form a line. Even though all forms of cluster initiation were grouped in this study, it is interesting to note that the average cluster area (168 km^2) compares with 104 km^2 reported by Huff (1987) for echoes with durations > 15 minutes.

Echo summary outputs provide several parameters; those parameters appear in Table 1. Maximum echo height is determined by the midpoint height (MSL) of the radar bin volume for the bin of greatest height with reflectivity > 20 dBz. Earth curvature and atmospheric refraction are included in the height calculation. The Area-Time-Integral is determined by multiplying the area enclosed by the 25 dBz contour by the centered time interval between the previous and the following scan. For the first scan, the time interval is one-half of the time increment between the initial scan and second scan; for the final increment, it is one-half the period between the last two scans. The product of area > 25 dBz and time is summed over the lifetime of the cluster; the sum is the Area-Time-Integral (Doneaud et al., 1984). Parameter RERV is the radar estimated rain volume as computed by using a Z-R relationship ($Z = 155R^{1.88}$, Smith et al., 1975). A rain rate is determined for each reflectivity recorded at the low-tilt elevations. The rain rate is multiplied by the projected area of the radar range bin and the time increment between scans. The product is summed for all bins for each scan for the lifetime of the cluster to get rain volume for the event.

The last four entries of the table are derived from soundings and are wind speeds based on soundings from one of six stations (Miles City, Baker, Colstrip, Knowlton, Powderville, and Glendive). The selected sounding was taken nearest in time (preceding the first echo time) and position to that of the cluster first echo. Wind directions at the surface, 850 mb, 700 mb, and 500 mb were included in the data set.

The range was bounded by a minimum of 20 km to a maximum of 200 km. Consideration of the beam characteristics implies that the nearest bin had a projected area of 0.18 km^2, while the most distant had a 1.74 km^2 projected area. This difference could be reflected in the data set as a range bias. From the radar parameters that were selected, maximum height is one of the parameters that should be influenced by a range bias.

The scatter plot of maximum echo height as a function of first echo range is presented in Fig. 1 to demonstrate a possible range bias. This figure indicates lower maximum heights in the 20 to 80 km range. This would indicate that the actual tops of the storms were not observed in this range interval because of the restricted scan elevations. At 12° elevation and 80 km range, the greatest echo height possible is 17.8 km, which is beyond the observed upper limit. For ranges greater than 140 km, the smaller events are missed; at maximum range, cloud tops must exceed 6.6 km to be observed. Echoes at long ranges require more development before satisfying the threshold because reflectivities for the larger bin volumes represent an average value for the total volume. This effect is substantiated by maximum reflectivity observations as well. Reflectivities do not exceed 60 dBz for ranges > 160 km; near 200 km, the maximum limit is nearer 55 dBz. For the parameters selected for study, only height will be directly affected by the bias at shorter ranges. Storm size (ATI, RERV, duration, and height) will average slightly above the true mean for large ranges. With these biases in mind, the following results are reported.

3. TYPICAL ECHO CLUSTER CHARACTERISTICS

Histograms of selected parameters are displayed in Figs. 2a-c. The central tendencies for these parameters are illustrated in Table 2. Figure 2a demonstrates the time-of-day frequency for first echo occurrence. The major peak between 1000-1100 occurs because of project design. Skywater radar began operations at 1000 whenever a "go" day was declared. Therefore, the percentage of "first echoes" at 1000 is artificially enhanced because earlier scans were not available and the first echo times were taken as the first scan time if the cluster was still growing. As expected, beyond the 1000 anomaly, the curve is somewhat bell-shaped with maxima occurring in the afternoon and evening. The mean and median of this distribution are the same and occur at 1518, while the mode is the 1000 block.

Frequency of storms as a function of day of the year is demonstrated in Fig. 2b. This histogram blocks the data by five-day segments and illustrates that there is great variability between the five-day groupings. It is interesting that the storms identified as significant events for case study analysis did not always occur during episodes of maximum storm frequency. Frequency extremes range from a low of 1.0% to a maximum of 14.6% and occur back-to-back around 24 July. An unusual event would be an entire five-day block without any storms, while it is not unusual for a five-day block to contain 10% of the summer events.

The typical echo cluster has a lifetime duration of 1.80 hour (distribution mean). Longest duration was over 10 hours. Some storms left the area during their lifetime and were not included in this study. This results in a bias decreasing the numbers of longer lasting storms. For storm motions of 12.5 m/s, durations of 9 hours or more are eliminated. The net effect of this bias is an accelerated frequency depression as a function of duration.

The distribution of maximum heights reached by echo clusters during their lifetimes is presented by Fig. 2c. The distribution is bimodal, centering about 6.9 and 9.4 km. The distribution is skewed to higher levels with 16.3 km being the highest observed. No cases were found to have maximum heights less than 4 km. The bimodal distribution is of interest and has also been observed by Braham (1981) during the METROMEX Project as given by the dashed line in the figure. Based on a numerical cloud model study by Mueller (1978), he attributed the bimodal distribution in cloud heights observed in the rural METROMEX population to the role of glaciation and cloud radius in allowing clouds to grow past mid-level dry layers. Small clouds are more strongly affected by mixing and thus are stopped by dry layers

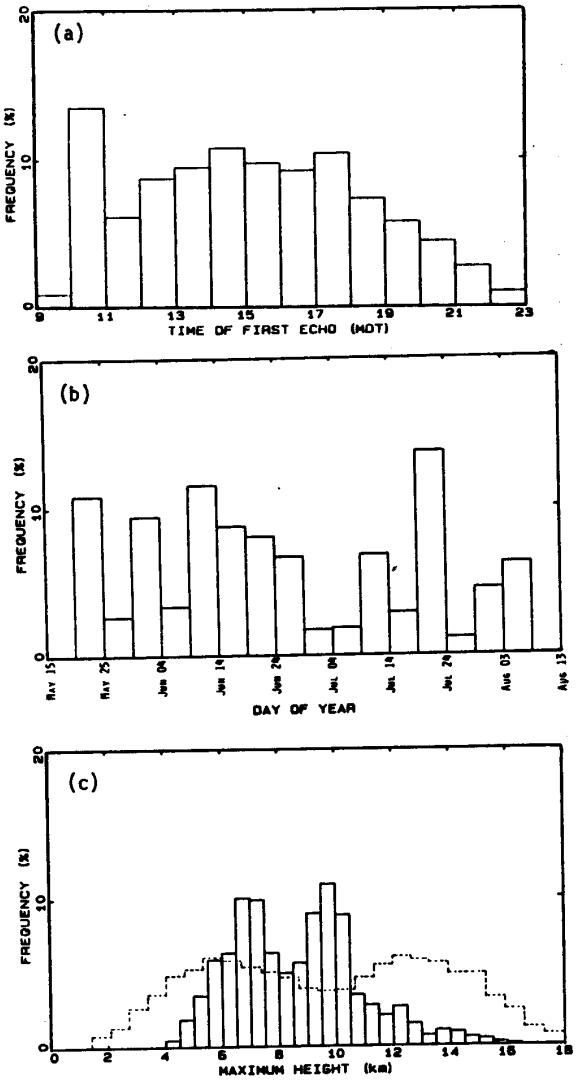

Fig. 2: Frequency histograms: a) Time of first echo using 1-hr bins to categorize the data set. On 17 July, operations started at 9:00 a.m., and these data are included in this figure for completeness. b) Occurrence of convective event by day of season using bins 5 days in width. The figure is extended with an empty block before 20 May and after 6 August to increase readability. c) Cluster lifetime maximum echo height using 1/2 km bin width. Dashed line for St. Louis clouds, adapted from Braham (1981).

aloft. Larger clouds are able to protect the updraft core from the effects of mixing with the dry mid-level environment and thereby continue to near the tropopause. Two modes are thus created: A low mode determined by the height of the mid-level dry layer and a high mode which is determined by the height of the tropopause. This may be a plausible hypothesis for the occurrence of the bimodal cloud height distribution in the CCOPE clouds.

TABLE 2

Measures of Central Tendency for Specific Parameters

	MEAN	MEDIAN	MODE	2σ RANGE	UNITS
Time of Day	15:18	15:18	10:02	12:02-18:34	hr (MDT)
Day of Year	175	170	202	152-199	day
Duration	1.80	1.33	0.51	0.4-3.2	hr
Maximum Height	8.4	8.2	6.9/9.4	6.2-10.6	km
Maximum Reflectivity	45.4	44.4	36.7	36.6-54.0	dBz
Radar Estimated Rain Volume	296†	284	1026	36.4-2406	km^2-mm
Area Time Integral	93.6†	80.0	22.4	13.9-628	km^2-hr
Average Range	123	125	124	82-164	km
Initial Range	122	125	193	73-171	km
Initial Azimuth	197	211	295	94-300	degree

†Mean of an assumed log normal distribution.

The radar reflectivity maxima (not shown) are distributed about a mean of 45.4 dBz and are skewed to lower values as indicated by a mode of 36.7 dBz. Reflectivities range from the threshold to a maximum of slightly over 67 dBz. About 17% of the cases reached maximum reflectivities exceeding 55 dBz, which has been shown by numerous investigators to be a reasonable indicator of the presence of hail (Dennis et al., 1971; Foote et al., 1979).

Radar rain volume estimates range from 1.1 to 168973 km^2-mm (km^2-mm = 1 metric kiloton) with both extreme events occurring on 31 May. The average is 296 km^2-mm which implies that the typical storm produces little moisture; only 6.3% of the events produced amounts > 10,000 km^2-mm. Half the total rainfall (922821 km^2-mm) was produced by 3% of the 765 clusters.

3.1 Cluster motion

A companion study of the CCOPE radar data resulted in an M.S. thesis by Tao (1987) which primarily dealt with cluster motion. The results of his study are summarized in Table 3. Mr. Tao's procedure was to subdivide the season into six time periods; this is the vertical presentation of the table. The horizontal extent of the table represents the eight cardinal directions of tracks taken by clusters. The numbers represent the percent of all clusters for a given time period that had trajectories from the given direction. The final table entry is the composite for the season.

The first time period, 20-31 May, indicates that cluster trajectories swept across the CCOPE network from the directions of north through east to southwest with no occurrences moving from the directions west to northwest, the highest frequencies of storm movement being from the southeast and southwest. The speeds were lower in the first period than for the rest of the season. The next time period (1-15 June) demonstrates a dramatic shift with trajectories preferring a west to east movement. This preference continues throughout the season except for the 1-15 July period when the southwest direction was slightly favored.

TABLE 3

Frequency of the Direction of Cluster Motion†

	No.	N	NE	E	SE	S	SW	W	NW	SPEED (m/s)
May 20-31	146	9	9	7	36	11	28			4-12
Jun 1-15	191					4	29	50	17	12-14
Jun 16-30	169			3	1		14	62	20	11-18
Jul 1-15	102				4	5	62	29		11
Jul 16-31	206						6	84	10	10-11
Aug 1-6	87						26	65	9	12-14
Season		1	1	2	7	3	28	48	9	10-18

†Based on Tao (1987). Motion is from the direction given similar to that used to describe wind direction. Last entry is the season summary.

This dominance of west to east trajectories during the summer months is as expected (Kuo and Orville, 1973). Typical cluster trajectories for the 1981 season are from the southwest or west at a speed of 12.5 m s^{-1}. Mean speed is uniform across all time periods except for May when the mean speed was 7 m s^{-1}. The transition from winter-spring weather systems to summer weather patterns which occurs near the end of May has a drastic effect on echo-cluster trajectories. This record indicates that this occurred toward late May or early June.

3.2 Parameteric variation during the day

Several of the parameters were reduced to hourly averages over the course of the project. For example, all measurements of duration for echo clusters that have a start time between 1000-1100 are averaged and illustrated in Fig. 3a by a point at 1000. Continuing this averaging technique for succeeding hours resulted in Fig. 3a. The averages tend toward the 1.8 hour overall mean with shorter durations for echo clusters starting later in the day. By project design, echo clusters starting late cannot have a long measured lifetime, yet storms that begin in the late evening may be inherently small and short-lived. Unfortunately, this comparison is incapable of discrimination between the two causes.

Hourly average maximum height is demonstrated in Fig. 3b. The greatest average maximum height of all echo clusters occurred for events with starting times after 2000 in the evening. There is a tendency for the maximum heights to increase throughout the day with a downward deflection around 1900. It has been documented that there's an early-evening resurgence of activity in this region (Koscielski and Dennis, 1976; Miller and Smith, 1986). The final two points could be contaminated because clusters that lasted longer than the surveillance time could not be included. Maximum reflectivity hourly averages (not shown) scatter about the mean (45.3 dBz), with lower values (43 dBz) for the morning period (1000 to 1200). The highest hourly averages occur in storms that start at 1700 (48.1 dBz) and 2100 (47.7 dBz). The estimated rain per cluster was also averaged by hour and the mean of 296 km^2·mm is followed by 9 of the 12 hourly intervals; the other 3 intervals (17, 20, 21 hrs) are well

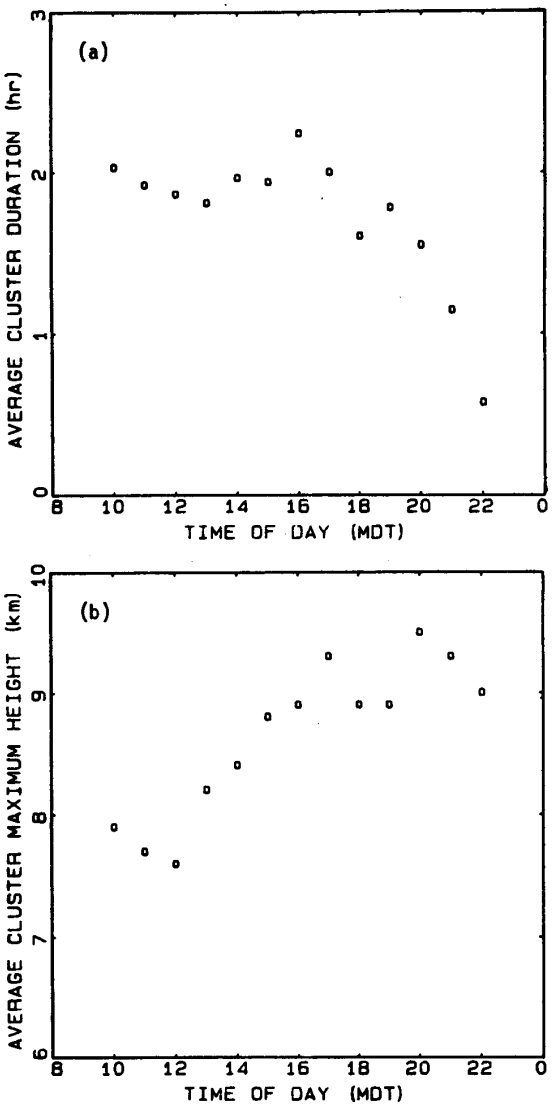

Fig. 3: Project hourly averages plotted against time of day: a) Cluster duration (r = -0.71); b) Cluster maximum height (r = 0.88).

above this value. Cluster rainfall hourly averages range from a low of 153 km^2·mm at 1200 to a high of 688 km^2·mm at 2100. The trend is for larger amounts of rainfall as the day progresses, as indicated by regression which resulted in a slope of 30.8 km^2·mm/hr (r=0.75). Storms that begin in the late afternoon and evening produce the most rain.

3.3 Seasonal influence

As previously demonstrated by Fig. 2c, echo cluster maximum height had a wide bimodal distribution with well-defined modes of 6.9 km and 9.4 km. When an average maximum height is considered for each day and plotted as a function of date, Fig. 4 results. Considerable scatter exists, yet there is a tendency for higher clouds

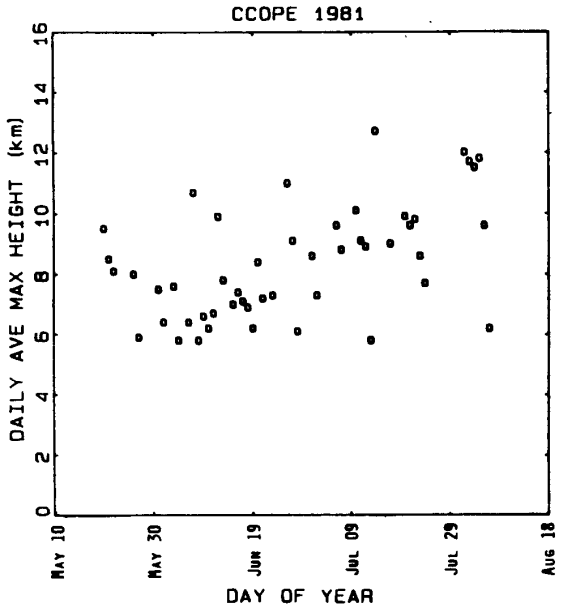

Fig. 4: Scatter plot of daily averaged cluster maximum height against day of year (r = 0.51, slope = 0.042 km/day).

with advancement of the year. The correlation coefficient is 0.51 and the slope is 0.042 km/day.

Using a similar averaging technique, several other parameters were followed throughout the summer season. The daily averaged echo duration is scattered about the mean with no substantial trend (r = -0.16, slope = -0.004 h/day). Since echo height increases through the season, it would be suspected that reflectivities would as well. Daily averaged maximum reflectivities result in a correlation of 0.28 and a slope of 0.059 dBz/day. Radar estimated rain volume daily averages indicate that these later-season storms do not produce a disproportionate amount of rainfall, no tendency is apparent, the correlation being 0.02 and the slope 0.001 km^2•mm/day. In summary, events early in the summer last slightly longer and may be less intense than events later in the year. The rainfall per event remains fairly constant throughout the season.

3.4 Parameters that influence rainfall

The longer an echo cluster exists, the greater the opportunity for rainfall to occur; duration should therefore be directly correlated to rainfall. Figure 5a demonstrates the scatter plot of duration to radar estimated rain volume (log scale). Indeed, the overall relationship supports this supposition (r = 0.75). Yet, when one considers the scatter, an event that lasted only one hour produced a rain volume of close to 10,000 km^2•mm, while another echo cluster that existed for an hour produced < 10 km^2•mm of rain. Thus there are huge differences in the absolute quantity of rain that falls for any given duration. There is also a noticeable curvature in the scatter plot suggesting that the relationship is actually nonlinear.

A plot of maximum height versus rain volume is presented in Fig. 5b and, as expected, there is a tendency for taller clouds to produce greater radar estimated rainfall. Maximum height is not a high confidence measure of rainfall, as one cluster with a maximum height of > 10 km yielded < 10 km^2•mm while another event with maximum height of about 6 km exceeded 10,000 km^2•mm rainfall. Generally, however, the larger rainfall storms are also the taller storms; the statistics yield a correlation of 0.65 and a standard log error of 0.694. Another parameter which trends with height is maximum reflectivity. Maximum reflectivity is compared to radar estimated rain volume in Fig. 5c. This results in a correlation of 0.80 and a standard log error of 0.55. The indication is that rainfall over the lifetime of the storm is proportional to maximum reflectivity.

Consistently strong correlations have been found for the comparison of ATI to RERV by Doneaud et al. (1984) for data collected during field projects in North Dakota. A similar correspondence was reported by Lopez et al. (1983, 1989) for Florida. The ATI comparison to RERV for CCOPE is presented in Fig. 5d. The relationship is very similar to those found in North Dakota. Using this relation for an estimation of rainfall results in a power law that can be represented by $V = K\ ATI^b$, where V = total rain volume, and K and b are constants of proportionality to be determined. The values of the multiplier K and the exponent b which have been determined for several projects are listed in Table 4. The multiplier K represents the average rain rate (mm/hr) for all echo clusters for the project. The exponent (b) being near one indicates that ATI values are additive, such that rainfall for composite events can be estimated as well.

The data set was subdivided by the 8 cardinal wind directions as a function of 4 heights (or pressures) observed by the proximity soundings at cluster initiation time, for a total of 32 possible categories. The frequency distribution of ambient wind direction at specific heights connected with cluster initiation is demonstrated by Table 5. At the surface, there is an obvious trend for wind directions at initiation time to be west through north and a secondary max for winds from the south. At the 850 mb level, the trend is still striking in the west/north sector and a secondary peak exists for south/southeast winds. Going to higher levels, the predominant wind nearly always has a westerly component exhibiting nearly zonal flow.

The possibility of terrain and surface inhomogeneity influences on first echo locations in the CCOPE area has been identified (Smolarkiewicz and Clark, 1985; Auer and White, 1983; Klitch and Vonder Haar, 1982). Further studies are investigating the possible relationship of observed FE locations to topographic features.

4. COMPARISONS WITH OTHER STUDIES

Comparison with other studies is made possible by the use of Table 6, which is comprised of average values that have been reported for other projects. One useful comparison would be with data from the North Dakota Cloud Modification Project in 1981. Comparing these two columns, CCOPE had first echoes that started 40 minutes

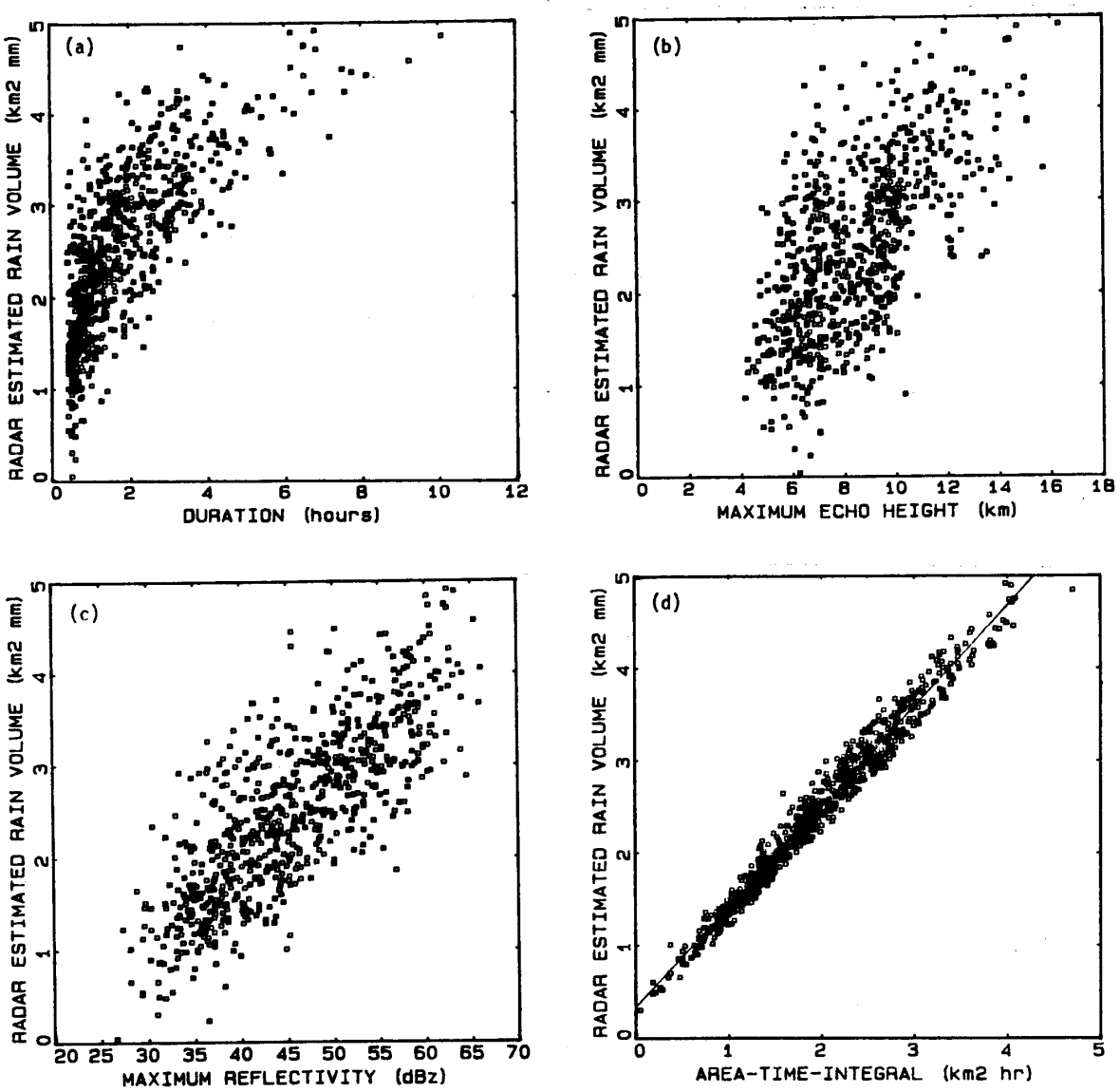

Fig. 5: Scatter plots against the log of radar estimated rain volume: a) Duration (r = 0.75, slope = 1.155 km^2•mm/hr). b) Cluster maximum height (r = 0.65, slope = 1.591 km^2•mm/km). c) Cluster lifetime maximum reflectivity (r = 0.80, slope = 7.54 km^2•mm/dBz). d) Log of Area-Time-Integral (r = 0.987, slope = 0.896 km^2•mm/km^2•hr).

earlier than those in North Dakota and lasted about 12 minutes longer. Maximum echo height was 1.4 km lower and maximum reflectivity about the same. The radar estimated rainfall difference of 54 km^2•mm with ND larger is opposite to that in storm size (CCOPE 40 km^2 greater in area). Being larger, yet producing less rain, would require the average rain rate be less for CCOPE clouds, and it is by 1.2 mm hr^{-1}. The ATI remains comparable.

The North Dakota 1982 comparison shows that CCOPE echo initiation time was 1:40 hours earlier, yet height and maximum reflectivity are much the same. Estimated rain volume is reduced by half for North Dakota, 1982; this reduction is also seen in the ATI value. Differences between ND 81 and 82 for the same area are greater than differences between CCOPE and ND 81.

Comparison to other projects is not quite as straightforward but is attempted in Table 6. Radar beam characteristics, project surveillance methods, parameter definitions, and reported stratifications are some of the conflicts that arise in such comparisons. Other projects that report a first echo beginning time indicate ~1 hour later initiation. Duration is not as easy to compare as the size criteria for cluster

TABLE 4

Rainfall Estimation Based on Area-Time-Integral

PROJECT	K (mm/hr)	b	r	RMS LOG ERROR
NDPP-1972†	2.62	1.09	0.97	0.16
NDCMP-1980*	3.68	1.01	0.98	0.17
NDCMP-1981*	3.07	1.08	0.98	0.16
Florida (1979-1981)††	3.4	1.0		
CCOPE-1981	2.133	1.086	0.987	0.147

†Doneaud et al., 1981.

*Doneaud et al., 1984.

††Lopez, 1989.

TABLE 5

Frequency Distribution (%) of Echo Clusters as a Function of Wind Direction at the Indicated Height for the Eight Cardinal Directions

	N	NE	E	SE	S	SW	W	NW
Surface	23.3	3.7	7.2	7.4	15.3	7.5	13.4	22.1
850 mb	12.7	2.4	6.3	16.0	11.1	6.7	19.0	25.8
700 mb	5.8	0.4	0.4	6.7	12.5	18.4	43.9	11.8
500 mb	4.5	0	3.4	2.5	3.4	21.3	61.8	3.0

definition changed between projects. NHRE and METROMEX report comparable durations of 50 minutes to an hour, while the Illinois projects reported duration of only 25 minutes. Data for Florida echoes lasting 1 hour were chosen for inclusion in Table 6 as most likely to be comparable.

Maximum height appears comparable in most regions, except for the western Nebraska and the NHRE projects, which were designed to study large hailstorms. This is further borne out by the average maximum reflectivity of 57 dBz reported for NHRE. Rain volume estimates vary in the same area from year to year (note North Dakota 1981 and 1982) by a factor of three. It is evident that southeastern Montana and northwestern North Dakota tend to produce less rainfall per event than the Midwest (Illinois and St. Louis). At the same time, the clouds producing the rain in the northern Great Plains are greater in areal extent. Florida demonstrates the smallest clouds in the comparison. Very few average rain rates were available, but the higher rates in Illinois would explain more rain from smaller clouds than seen in the northern Great Plains, as expected from the greater moisture available.

5. CONCLUDING REMARKS

In conclusion, we find a general consistency of the results described in this study with those of North Dakota 1981. This suggests that these results are applicable to the broader northern

TABLE 6

Parametric Mean Value Comparisons with Other Projects

	CCOPE	ND 81	ND 82	ILL	NHRE	ST. LOUIS	NEBR. HAIL	FLA
Initiation Time (hr:min)	15:18	~1600	~1700		1600	1700	1600	
Duration (hr)	1.8	1.6	--	0.4	0.9	0.8		1.0
Max Height (km)	8.4	9.8	8.6	8.6	10.7	8.6	11.4	9.4
Max. Reflec. (dBz)	45	44	41	38	57		45	40
Rain Vol. (km^2-mm)	296	350	131	548		1220		
Max Area (km^2)	168	128		104		114		92
Average Rain Rate (mm/hr)	3.16	4.4	3.5	9				
Depth (mm)						11.4		
ATI (km^2-hr)	93.1	80	32.8					
Total Area (km^2)				815				

Great Plains region. We note that the Smith et al. (1985) study indicates the potential for substantial year-to-year variation in echo statistics which is demonstrated by the North Dakota 1981-1982 comparison. This suggests that caution should be used in extrapolation of these results to other years. There are greater differences when compared with radar echoes from more humid environments.

To our knowledge, the bimodal distribution of maximum echo heights observed in the present study has not been reported previously for High Plains storms. The implications of the results of the modeling study by Mueller (1978) suggesting that METROMEX clouds could be moved from the lower mode to the higher mode as a result of enhanced glaciation are especially intriguing.

The usefulness of the Area-Time-Integral (ATI) in estimating total storm rainfall is reaffirmed for this data set. On the other hand, maximum echo height is found not to be as good an estimator of rainfall, as found in previous studies (Smith et al., 1985a, 1985b). Perhaps the better resolution provided by the 1° beamwidth of the Skywater radar data used here is a factor.

Finally, some of the time of day and seasonal trends can be useful in planning weather modification projects in the region.

Acknowledgments. Support of this research was provided by the National Science Foundation, Division of Atmospheric Sciences, under Grant ATM-8610159.

Special thanks are extended to Douglas Black, Greg Thesis, and Chris Kruschke for all their tedious efforts in processing the data. Thanks are also extended to Dr. Paul L. Smith for his scientific leadership and to Mrs. Sandra Palmer and Mrs. Joie Robinson for typing the manuscript.

REFERENCES

Auer, A. H., and J. M. White, 1983: Boundary layer perturbation associated with terrain, physiographical and topographical influences in CCOPE. Final Report, NSF Grant ATM-8107096, Dept. of Atmospheric Sciences, University of Wyoming. 57 pp.

Braham, R. R., Jr., 1981: Urban precipitation processes. In METROMEX: A Review and Summary. Meteor. Monogr., Vol. 18, No. 40, 76-116.

Dennis, A. S., P. L. Smith, Jr., E. I. Boyd and D. J. Musil, 1971: Radar observations of hailstorms in western Nebraska. Report 71-1, Institute of Atmospheric Sciences, S.D. School of Mines and Technology, Rapid City, SD. 42 pp.

Doneaud, A. A., P. L. Smith, A. S. Dennis and Sumedha Sengupta, 1981: A simple method for estimating convective rain volume over an area. Water Resources Research, 17, 1676-1682.

Doneaud, A. A., S. Ionescu-Niscov, D. L. Priegnitz and P. L. Smith, 1984: The area-time integral as an indicator for convective rain volumes. J. Climate Appl. Meteor., 23, 555-561.

Dye, J. E., J. J. Jones, N. P. Winn, T. A. Cerni, B. Gardiner, D. Lamb, R. L. Ritter, J. Hallett and C. P. R. Saunders, 1986: Early electrification and precipitation development in a small, isolated Montana cumulonimbus. J. Geophys. Res., 91, 1231-1247.

Fankhauser, J. C., C. J. Biter, C. G. Mohr and R. L. Vaughan, 1985: Objective analysis of constant altitude aircraft measurements in thunderstorm inflow regions. J. Atmos. Oceanic Technol., 2, 157-170.

Foote, G. B., R. E. Rinehart and E. L. Crow, 1979: Results of a randomized hail suppression experiment in northeast Colorado. Part IV: Analysis of radar data for seeding effect and correlation with hailfall. J. Appl. Meteor., 18, 1569-1582.

Huff, F. A., 1987: Summary of several radar echo studies for weather modification application in Illinois. J. Wea. Modif., 19, 82-91.

Klitch, M. A., and T. H. Vonder Haar, 1982: Compositing digital satellite data to detect regions of orographically induced convection on the northern High Plains. Paper No. 351, Dept. of Atmospheric Sci., Colorado State University, Fort Collins, CO. 87 pp.

Knight, C. A., and K. Knupp, 1986: Precipitation growth trajectories in CCOPE. J. Atmos. Sci., 43, 1057-1073.

Koch, S. E., R. E. Golus and P. B. Dorian, 1988: A mesoscale gravity wave event observed during CCOPE. Part II: Interaction between mesoscale convective systems and the antecedent waves. Mon. Wea. Rev., 116, 2545-2569.

Kuo, J-T., and H. D. Orville, 1973: A radar climatology of summertime convective clouds in the Black Hills. J. Appl. Meteor., 12, 359-368.

Lopez, R. E., J. Thomas, D. O. Blanchard and R. L. Holle, 1983: Estimation of rainfall over an extended region using only measurements of the area covered by radar echoes. Preprints 21st Conf. Radar Meteor., Edmonton, Alberta, Canada, Amer. Meteor. Soc., 681-686.

Lopez, R. E., D. O. Blanchard, D. Rosenfeld, W. L. Hiscox and M. J. Casey, 1984: Population characteristics, development processes and structure of radar echoes in south Florida. Mon. Wea. Rev., 112, 56-75.

Lopez, R. E., D. Atlas, D. Rosenfeld, J. L. Thomas, D. O. Blanchard and R. L. Holle, 1989: Estimation of rainfall using the radar echo area time integral. J. Appl. Meteor., 28, 1162-1175.

Koscielski, A., and A. S. Dennis, 1976: Comparison of first radar echoes in seeded and unseeded convective clouds in North Dakota. J. Appl. Meteor., 15, 309-311.

Miller, J. R., and P. L. Smith, 1986: Some characteristics of radar first echoes in the High Plains. J. Wea. Modif., 18, 95-101.

Miller, L. J., J. D. Tuttle and C. A. Knight, 1988: Airflow and hail growth in a severe northern High Plains supercell. J. Atmos. Sci., 45, 736-762.

Mueller, S. F., 1978: An application of the Simpson-Wiggert cloud model to METROMEX Hi-Cu data. Preprints Conf. Cloud Physics and Atmos. Elec., Issaquah, WA, Amer. Meteor. Soc., 490-495.

Rasmussen, R. M., and A. J. Heymsfield, 1987: The melting and shedding of graupel and hail: Part III. Investigations of the role of shed drops as hail embryos in the August 1 CCOPE severe storm. J. Atmos. Sci., 44, 2783-2803.

Schmidt, J. M., and W. R. Cotton, 1989: A High Plains squall line associated with severe surface winds. J. Atmos. Sci., 46, 281-301.

Schroeder, M. J., and G. E. Klazura, 1978: Computer processing of digital radar data gathered during HIPLEX. J. Appl. Meteor., 17, 498-507.

Smith, P. L., D. E. Cain and A. S. Dennis, 1975: Derivation of an R-Z relationship by computer optimization and its use in measuring daily areal rainfall. Preprints 16th Radar Meteor. Conf., Houston, TX, Amer. Meteor. Soc., 461-466.

Smith, P. L., J. R. Miller, Jr., A. A. Doneaud, J. H. Hirsch, D. L. Priegnitz, P. E. Price, K. J. Tyler and H. D. Orville, 1985a: Research to develop evaluation techniques for operational convective cloud modification projects. Report SDSMT/IAS/R-85/02, Institute of Atmospheric Sciences, S.D. School of Mines and Technology, Rapid City, SD. 93 pp.

Smith, P. L., A. A. Doneaud, J. H. Hirsch, J. R. Miller, Jr., and P. E. Price, 1985b: Development of evaluation techniques for operational convective cloud modification projects: 1984-85 studies. Report SDSMT/IAS/R-85/05, Institute of Atmospheric Sciences, S.D. School of Mines and Technology, Rapid City, SD. 34 pp.

Smolarkiewicz, P. K., and T. L. Clark, 1985: Numerical simulation of the evolution of a three-dimensional field of cumulus clouds. Part I: Model description, comparison with observations and sensitivity studies. J. Atmos. Sci., 42, 502-522.

Tao, Ningsheng, 1987: Some radar echo characteristics during CCOPE. M.S. Thesis, Dept. of Meteor., S.D. School of Mines and Technology, Rapid City, SD. 102 pp.

APPENDIX H

AN EXPLORATORY STUDY OF THE SUMMERTIME OBSERVATIONS BY A DUAL-WAVELENGTH MICROWAVE RADIOMETER AT DICKINSON, NORTH DAKOTA IN 1987

by

Valentine G. Anantharaj

A thesis submitted to the Graduate Division
in partial fulfillment of the requirements
for the degree of
MASTER OF SCIENCE IN METEOROLOGY

SOUTH DAKOTA SCHOOL OF MINES AND TECHNOLOGY
RAPID CITY, SOUTH DAKOTA

1989

Prepared by:

Valentine Anantharaj
Valentine G. Anantharaj

Approved by:

James R. Miller, Jr.
Major Professor

Harold D. Orville
Chairman, Department of Meteorology

1/24/90
Dean, Graduate Division

ABSTRACT

The DRI/NOAA Dual-wavelength, Mobile, Scanning Microwave Radiometer was deployed during the 1987 Federal/State Cooperative Program in Weather Modification at Dickinson, North Dakota to study the summertime convective clouds. The algorithm used for the retrieval of the integrated precipitable water vapor (IPWV) and the integrated liquid water (ILW) yields values of IPWV that correlate well with the precipitable water (PW) values integrated from radiosonde soundings. Nearly 6% of the available PW, calculated from the radiosonde data, are found to exist above the 500 mb level.

The average column vapor for the season was 2.13 cm with the maximum and minimum being 3.97 cm and 0.75 cm respectively. Continuous monitoring of the IPWV trends will be helpful in forecasting precipitation in the summertime. A rising trend in vapor over a period of 3 or 4 days resulted in precipitation. Also 5 out of 8 rainy days had averaged IPWV values greater than 2.5 cm.

The drying behind cold fronts after the passage could be observed using this instrument. The trends in the IPWV as observed by this instrument are different from the hourly observations of surface dew points, indicating that this instrument is capable of providing moisture information otherwise not obtainable from surface dew points.

Cloud scans at different elevation angles were conducted as oppurtunities were recognized. The accuracy of the values of IPWV and ILW in larger convective clouds becomes suspect in the presence of precipitation size particles due to scattering effects, which are neglected in the derivation of the retrieval algorithm. The approximations of the average liquid water concentration and water vapor mixing ratios in clouds are reasonable when good information about the cloud sizes was available. Additional information such as the profile of temperature through the clouds could help identify regions of supercooled liquid water. The cloud boundaries are identified by the rise in the values of IPWV and ILW over the clear sky measurements.

TABLE 1

First-Echo Height and Temperature (daily mean)
for Three Days in June 1987

Date	No. of Echoes	Minimum FEH (km)	Maximum FEH (km)	Mean FEH (km)	Standard Deviation (km)	0°C Level (km)	Temp. at Mean FEH (°C)
16	34	4.40	7.70	6.32	0.88	4.6	-14.0
18	64	3.70	6.60	5.00	0.54	4.0	- 6.0
22	67	3.50	8.50	5.98	1.11	4.95	-11.8
Composite							
	165	3.50	8.50	5.67	1.03		

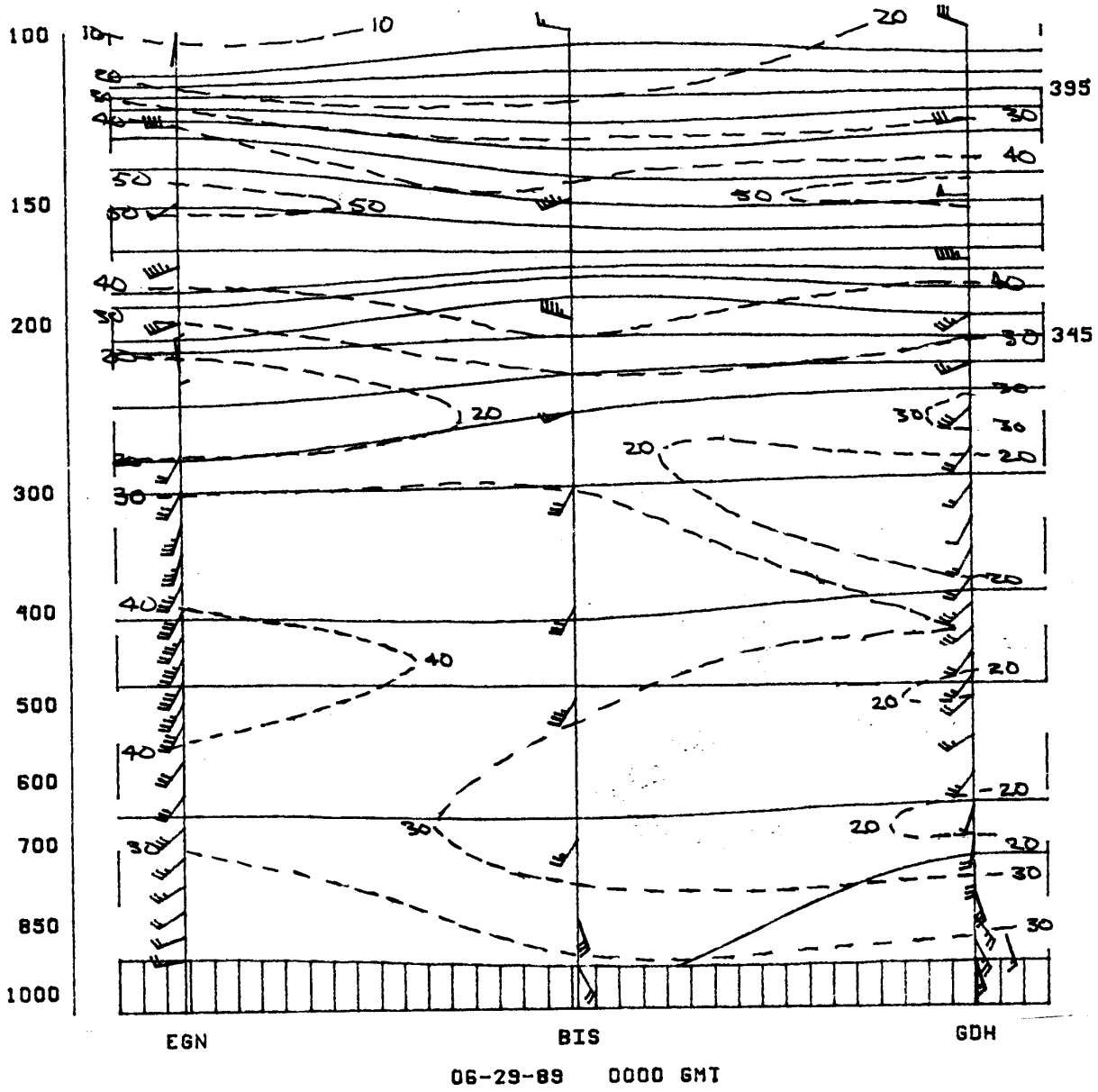
100
150
200
300
400
500
600
700
850
1000
395
345
EGN
BIS
GDH
06-29-89 0000 GMT

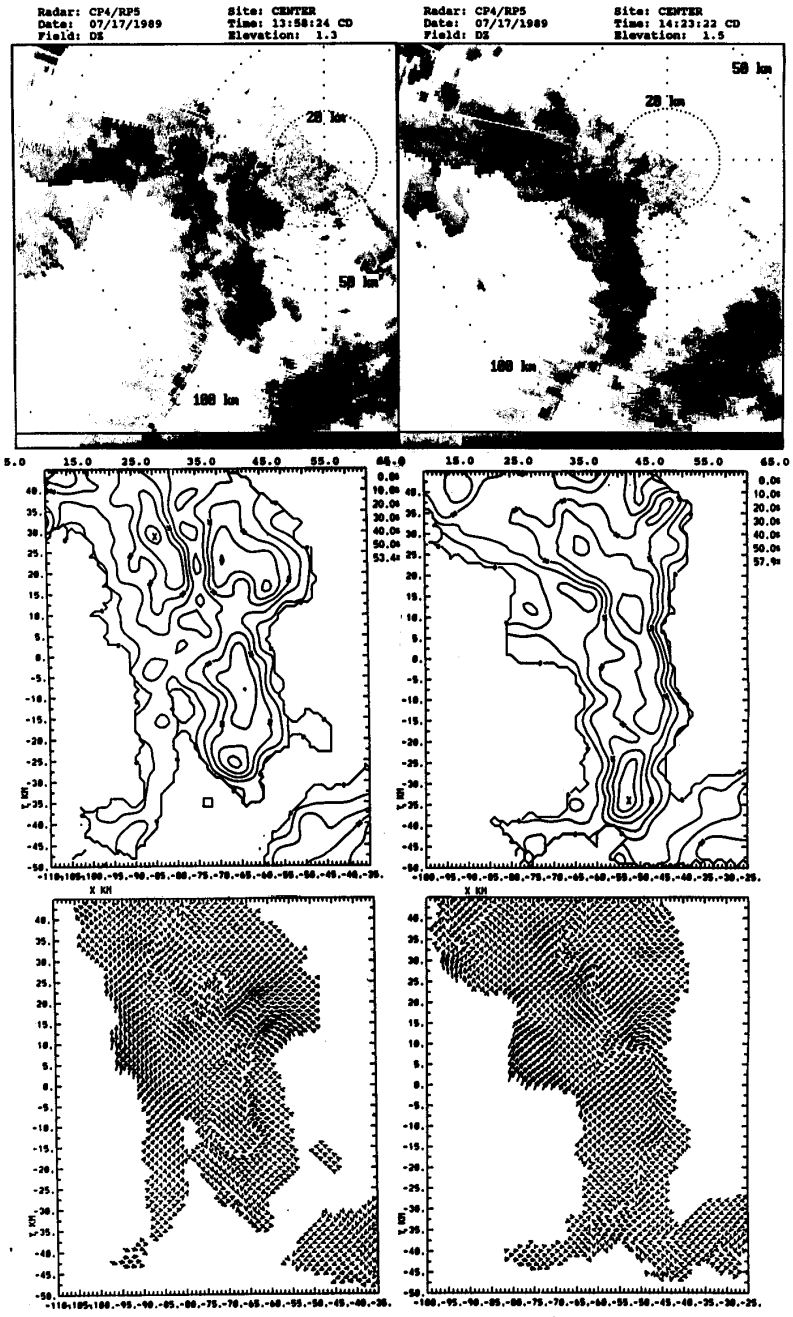
Radar: CP4/RP5
Date: 07/17/1989
Field: DZ
Site: CENTER
Time: 13:58:24 CD
Elevation: 1.3
Radar: CP4/RP5
Date: 07/17/1989
Field: DZ
Site: CENTER
Time: 14:23:22 CD
Elevation: 1.5
28 km
50 km
100 km
X KM
Y KM

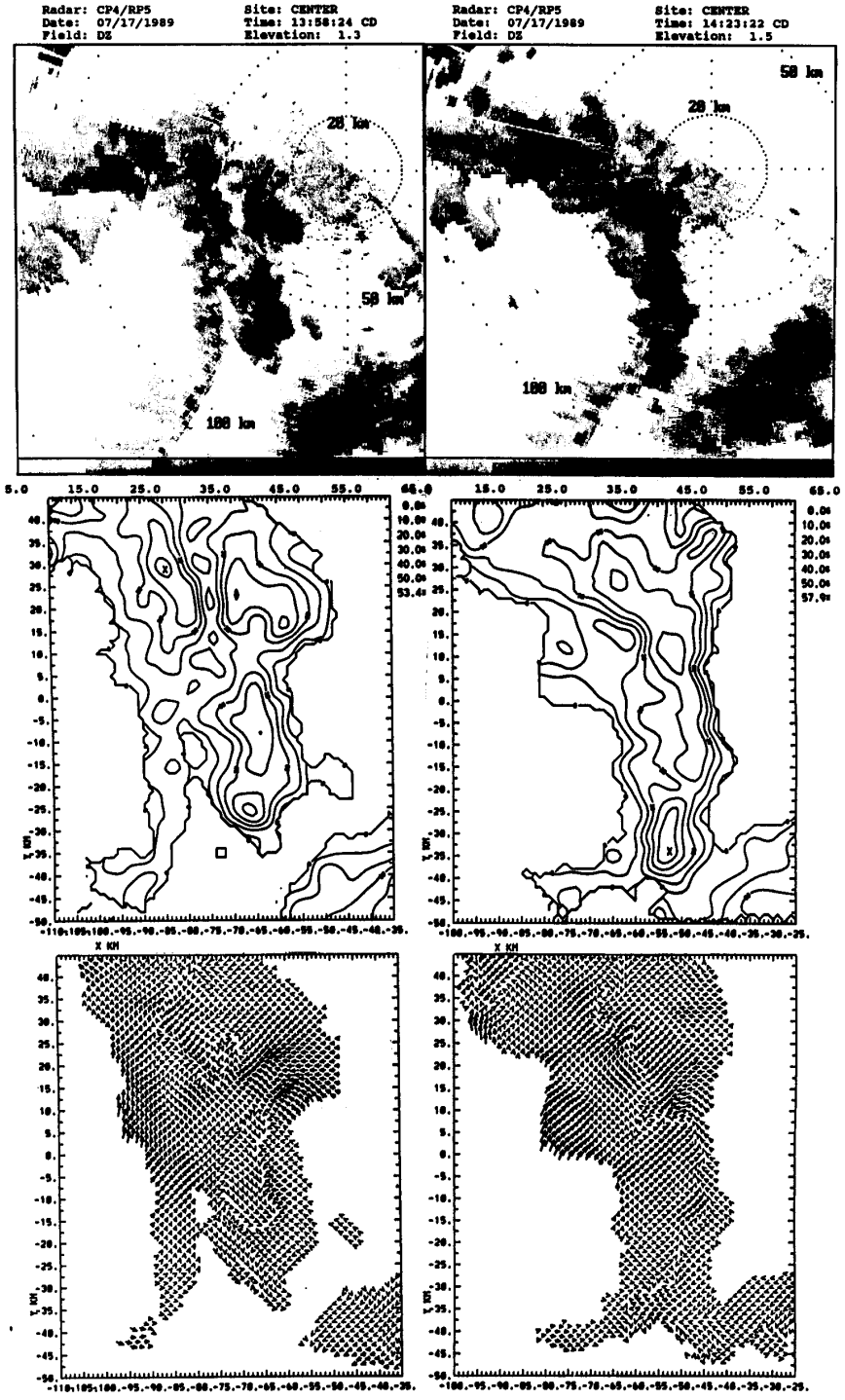
Radar: CP4/RP5
Date: 07/17/1989
Field: DZ
Site: CENTER
Time: 13:58:24 CD
Elevation: 1.3
Radar: CP4/RP5
Date: 07/17/1989
Field: DZ
Site: CENTER
Time: 14:23:22 CD
Elevation: 1.5
20 km
50 km
100 km
X KM
Y KM

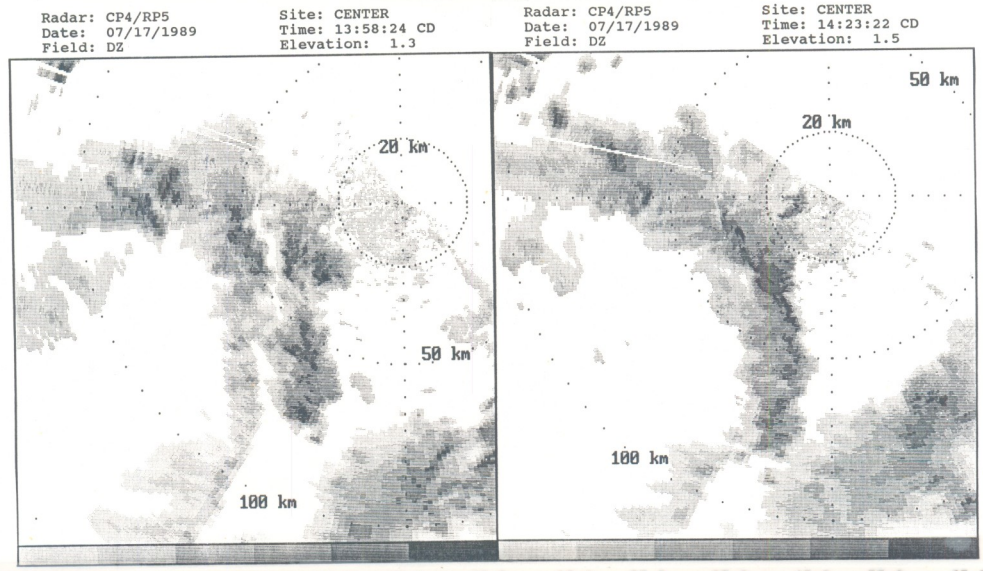
Radar: CP4/RP5
Date: 07/17/1989
Field: DZ
Site: CENTER
Time: 13:58:24 CD
Elevation: 1.3
20 km
50 km
100 km
Radar: CP4/RP5
Date: 07/17/1989
Field: DZ
Site: CENTER
Time: 14:23:22 CD
Elevation: 1.5
50 km
20 km
100 km

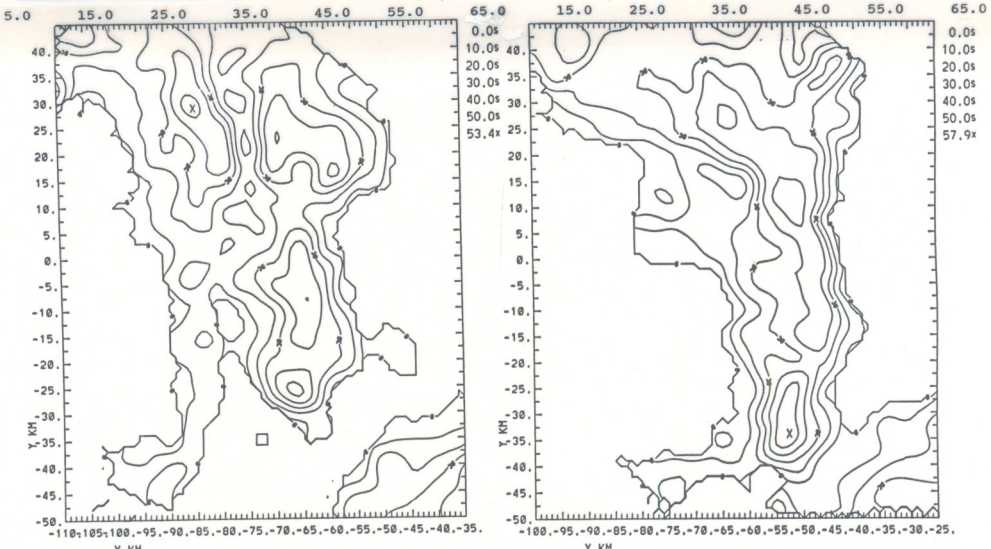
5.0 15.0 25.0 35.0 45.0 55.0 65.0
0.0s
10.0s
20.0s
30.0s
40.0s
50.0s
53.4x
Y, KM
-110.-105.-100.-95.-90.-85.-80.-75.-70.-65.-60.-55.-50.-45.-40.-35.
15.0 25.0 35.0 45.0 55.0 65.0
0.0s
10.0s
20.0s
30.0s
40.0s
50.0s
57.9x
Y, KM
-100.-95.-90.-85.-80.-75.-70.-65.-60.-55.-50.-45.-40.-35.-30.-25.

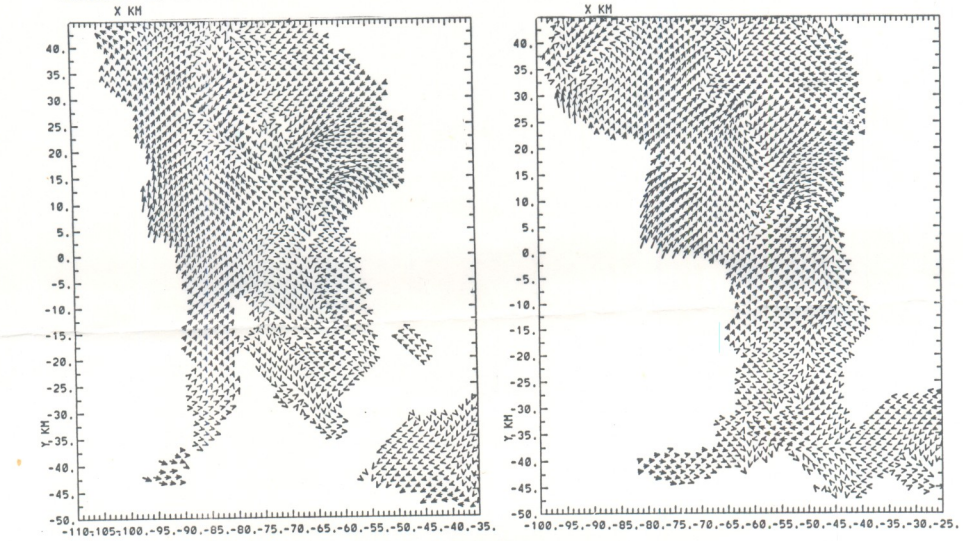
X KM
Y, KM
-110.-105.-100.-95.-90.-85.-80.-75.-70.-65.-60.-55.-50.-45.-40.-35.
X KM
Y, KM
-100.-95.-90.-85.-80.-75.-70.-65.-60.-55.-50.-45.-40.-35.-30.-25.